Regular Article

Investigation of $\Xi^- nn$ ($S = -2$) hypernucleus in low-energy pionless halo effective theory

Ghanashyam Meher[a] and Udit Raha[b]

Department of Physics, Indian Institute of Technology Guwahati, Guwahati, Assam 781 039, India

Abstract We study the $\Xi^- nn$ ($S = -2$, $I = 3/2$, $J^P = 1/2^+$) three-body system using low-energy effective field theory (EFT). Due to the acute inadequacy of empirical information in this sector, there exists substantial degree of ambiguity in determining various few-body observables, some of which are expected to yield vital clues to resolving longstanding contentious issues in hypernuclear physics. Moreover, in astrophysical studies, a precise determination of neutron star equation of state (EoS) of putative hyperonic cores relies on essential input from the $S = -2$ sector. In this obscure current scenario, a pionless EFT analysis provides a systematic model-independent framework for assessing the feasibility of light three-particle-stable bound states, utilizing low-energy universality. Here we take recourse to a simplistic speculation of the three-body system by eliminating the repulsive spin-singlet $\Xi^- n$ sub-system, while retaining the predominantly attractive (possibly bound) spin-triplet $\Xi^- n$ and the virtual bound spin-singlet nn sub-systems. In particular, a qualitative leading order EFT investigation by introducing a sharp momentum ultraviolet cut-off parameter $\Lambda_{\rm reg}$ into the coupled integral equations indicates a discrete scaling behavior akin to a renormalization group limit cycle, thereby suggesting the formal existence of Efimov states in the unitary limit, as $\Lambda_{\rm reg} \to \infty$. Our subsequent non-asymptotic analysis indicates that the three-body binding energy B_3 is sensitively dependent on the cut-off without the inclusion of three-body contact interactions. Furthermore, our analysis reproduces several values of the binding energy $B_3 \sim 3-4$ MeV, predicted in context of existing potential models, with the regulator $\Lambda_{\rm reg}$ in the range $\sim 350-460$ MeV. Finally, based on these model inputs for B_3, a ballpark estimate of the three-body scattering length in the range $2.6-4.9$ fm, is naively constrained by our EFT analysis. Despite approximations, the resulting Phillips line is expected to yield a robust feature of the halo-bound $\Xi^- nn$ system. For pedagogical reasons, using a simple toy model interacting three-bosons system, we highlight in the appendices the typical universal features leading to emergence of RG limit cycle and Efimov states which are amenable to a low-energy EFT formalism.

1 Introduction

The physics of hypernuclei has gained considerable attention in the strangeness nuclear physics community through numerous studies of exotic hypernuclei (for recent reviews, see, e.g., Refs. [1–6]). Such studies have also proven to have important consequences in the astrophysics of neutron stars where strange matter is expected to appear at their cores (e.g., see Refs. [7–9]). Especially, the strangeness $S = -2$ sector has engendered for a long time a great deal of activity behind ideas, such as the existence of the putative H-dibaryon and other light Ξ-hypernuclei, or to seek a resolution to the well-known hyperon puzzle [10,11]. For instance, with regard to the feasibility of the H-particle, as conjectured by Jaffe more than 40 years ago [12], no definite conclusion has been reached

till date, despite the extensive theoretical [13–26] and experimental investigations [27,28]. It has been recognized that a thorough understanding of the role and character of the underlying YNN and YYN three-body forces (3BFs) is vital towards resolving some of these contentious issues. Especially, to stabilize neutron stars with masses larger than twice the solar mass ($2M_\odot$) against gravitational collapse, the sole inclusion of NN, YN, and YY two-body interactions becomes questionable, as they lead to considerable softening of the equation-of-state (EoS) [29] of the dense baryonic matter. The answer probably lies in the inclusion of an admixture of NNN, ΛNN, $\Lambda\Lambda N$ and ΞNN 3BFs that may be the key in estimating the correct stiffness of the EoS governing the stability of the cores. Notably, the Quantum Monte Carlo simulations by Lonardini et al. [30,31] have already shown encouraging indication that the inclusion of ΛNN 3BF compensates the excessive overbinding due to the ΛN interactions, ostensibly resolving the "B_Λ-overbinding" problem. Further work

[a] e-mail: ghanashyam@iitg.ac.in
[b] e-mail: udit.raha@iitg.ac.in (corresponding author)

in this direction is necessary for a comprehensive understanding of the 2017 observation of gravitational waves from two-neutron star mergers by the LIGO Scientific Collaboration [32].

In 2001, the NAGARA event [33] from the KEK E373 emulsion experiment undoubtedly provided the first evidence of the light double-Λ hypernuclei $_{\Lambda\Lambda}^{6}\text{He}$, demonstrating that the $S = -2$ $\Lambda\Lambda$ interactions are less attractive than the $S = -1$ ΛN counterparts. On the other hand, the feasibility of a light Ξ-hypernuclei based on the state-of-the-art experimental [34–36] and theoretical [37–45] studies remains largely equivocal since they were first claimed in 1959 in the experimental work of Wilkinson et al. [46]. This is primarily due to the acute scarcity of $S = -2$ empirical information[1] needed to determine the underlying character of the hypernuclear interactions. All that one finds in the literature are a few scattered upper bounds for $\Xi^- p \to \Xi^- p$ (elastic) and $\Xi^- p \to \Lambda\Lambda$ (inelastic) cross sections from emulsion experiments [49–51] for laboratory frame momenta in the range $500-600$ MeV. Thus, it is no surprise that different existing model analyses lead to substantially contrasting views regarding the nature of the ΞN potentials, ranging from moderately or weakly attractive [34,44,49–57], even vanishing [58], to weakly repulsive [59]. In fact, the KISO event [36] from the KEK E373 experiment in 2015, which undeniably confirmed the particle-stable Ξ-hypernucleus $_{\Xi}^{15}\text{C}$ (interpreted as the ground state of a deeply bound $\Xi^- - ^{14}\text{N}$ cluster system with binding energy 4.38 ± 0.25 MeV), at the least corroborated that the constituent ΞN channels are attractive. Specifically, the updated (*Extended-soft-core* ESC08c) Nijmegen model G-matrix analyses [60,61] have predicted that the ΞN two-body system in the maximal spin–isospin ($i = 1, j^p = 1^+$) channel is strongly attractive and forms a near-threshold bound state with large positive $^3S_1$ scattering length, namely, $a_{\Xi n}^{(j=1)} = 4.911$ fm. On the contrary, the ($i = 1, j^p = 0^+$) channel was predicted to be predominantly repulsive with small $^1S_0$ scattering length, namely, $a_{\Xi n}^{(j=0)} = 0.579$ fm. Using a potential model involving Faddeev equations, the putative two-body bound state in the former attractive ΞN channel, so-called the deuteron* (D^*), was estimated to have a binding energy of 1.56 MeV (1.67 MeV) by (without) taking into consideration the latter repulsive ΞN channel [42,43]. In a contrasting scenario, the recent SU(3) chiral effective field theory (EFT) predictions from the relativistic leading order (LO) analysis of Ref. [56], as well as the non-relativistic *next-to-leading order* (NLO) *in-medium* G-matrix analysis of Ref. [57], have practically ruled out the possibility of a particle-stable ΞN bound state in the (1,1) channel. It is noteworthy that both EFT analyses were constrained by the recent HAL QCD lattice results [62] and the aforementioned empirical upper bounds from $\Xi^- p$ cross sections data [49–51,55]. Interestingly, the recent Faddeev calculations [6,26,39,41–43] relying either on the updated ΞN Nijmegen ESC08c potential model [60,61] as input for the $I = 3/2, J^P = 1/2^+$ channel, or on the recent HAL QCD-based $\Lambda\Lambda - \Xi N$ separable interaction potential [62] as input for the $I = 1/2, J^P = 1/2^+$ channel, have hinted at the feasibility of a deeply bound ΞNN state in the former channel and a three-body $\Xi NN - \Lambda\Lambda N$ resonance state (i.e., either as a $\Lambda\Lambda N$ resonance state or a ΞNN quasi-bound state) in the latter.[2] These facts ostensibly imply that the ΞN interactions are predominantly attractive in nature.

2 Pionless EFT ($\not{\pi}$EFT): a brief survey

Prompted by this unresolved scenario, we present in this work an alternative qualitative assessment regarding the viability of a putative $\Xi^- nn$ two-neutron halo-bound state in the $I = 3/2, J^P = 1/2^+$ channel. In particular, the reasons motivating our study of the ΞNN system in this maximal spin–isospin channel are as follows:

– First, the decoupling of this channel from the strong decay into the $\Lambda\Lambda N$ channel is forbidden by isospin conservation.[3]

---

[1] Due to the current impracticability of Ξ-hyperon scattering experiments, accurate data is difficult to procure. However, study of pertinent correlations in heavy-ion collisions or highly energetic proton-proton scattering in future facilities like ALICE and PANDA could certainly improve the present scenario [47,48].

---

[2] Even a contrasting viewpoint is obtained in the ΞNN system in the light of the more recent variational calculation using Gaussian expansion method [44] with Nijmegen ΞN potential [60,61]. Oddly enough, their findings indicate a rather strongly attractive $I = 1/2, J^P = 1/2^+$ channel with a three-body bound state with binding energy 7.20 MeV, while the $I = 3/2, J^P = 1/2^+$ channel is less attractive without a bound state.

[3] The ΞNN system in the $I = 1/2, J^P = 1/2^+$ channel, on the other hand, has profound astrophysical importance in the context of EoS of neutron star matter. It has been recognized that $\Xi NN \to \Lambda\Lambda N$ transmutations could contribute to an intricate balance between the ordinary nucleonic and hyperonic matter accumulating at the stellar cores, inducing a natural "pressure control" mechanism for the build-up of neutron and lepton Pauli pressures in high-density matter. Moreover, the ΛNN and $\Lambda\Lambda N$ three-body observables can additionally serve to fine-tune the stiffness of the EoS in a controlled way. In this regard, a series of chiral constituent quark model analyses by Garcilazo el al. [63–65] using Faddeev equations suggested the importance of $\Xi NN - \Lambda\Lambda N$ couplings in obtaining a three-body bound state, so-called the $S = -2$ hypertriton (with binding energy ~ 0.5 MeV), given that the $\Lambda\Lambda N$ system is by and large unbound. However, such a bound state mechanism seems fundamentally at odds with Efimov universality, since the feasibility of Efimov states gets substantially weakened or disappears in proximity to open decay or reaction channels [66,67]. Thus, it seems rather unlikely that the above reported bound state is manifestly Efimov-like in character. This calls for a rigorous

– Second, Pauli principle works favorably in supporting stable ΞNN bound states.
– Third, the absence of Coulomb effects to a great extent simplifies the EFT construction of the coupled integral equations in the momentum-space [68], the so-called STM or Skornyakov–Ter-Martirosyan equations [69–71] (cf. Appendix A.2).

Our treatment is based on a low-energy pionless EFT ($\not{\pi}$EFT) [68,72–83] where explicit pion exchanges are integrated out at scales much smaller than the pion mass. A speciality of such an approach is that the results are obtained following a general model-independent perturbative scheme utilizing principles of low-energy universality with controlled error estimates. Observables are expressed as an expansion of a small low-energy parameter $\epsilon = Q/\Lambda_H$, with Q being the typical momentum scale of dynamics of the system in question, and $\Lambda_H \sim m_\pi$ is the hard or breakdown scale of the theory which is identified with the pion mass m_π. Such a methodology is complementary to ab initio approaches, where the universal phenomenological couplings or low-energy constants (LECs) in the effective Lagrangian could be used to make predictions on various few-body observables. Such universal aspects of $\not{\pi}$EFT have been successfully exploited to investigate the dynamics of finely tuned systems of atoms and light nuclei driven arbitrarily close to the unitary limit of two-body short-distance interactions. This is either achieved *artificially*, by tuning inter-atomic potentials in selective open channels using varying electromagnetic fields, as in Feshbach resonances [68] in ultra-cold atoms, or even *naturally*, as in nuclear systems with large two-body scattering lengths. This leads to formation of threshold two-body bound states, such as in the case of the deuteron (np bound state) or in our context of the aforementioned putative bound D^* state [60,61]. More interestingly, interacting three-body S-wave systems when driven in proximity to the unitary limit, lead to the well-known Efimov phenomenon [68,84–90], associated with an infinite tower of arbitrarily shallow geometrically spaced three-body levels accumulating to zero-energy, namely, the three-particle or particle-dimer break-up threshold (see, e.g., [2,68,90] and reference therein for a detailed review of Efimov physics and its applications in atomic and nuclear physics). In that case a modified $\not{\pi}$EFT power counting scheme was suggested by Bedaque et al. [72,73]. The power counting mandates non-derivative three-body contact interaction couplings, which are otherwise subleading in a *naive* dimensional analysis (NDA), to be promoted to the LO whenever they exhibit renormalization group (RG) limit cycle. For pedagogical purpose, Appendix A highlights brief technical details of the $\not{\pi}$EFT formalism capturing the two- and three-body universal physics relating to Efimov-like bound states. A simple toy model analysis of a system of

three identical interacting bosons provides the essential background for the methodology adopted in this paper.

An important variant of the standard $\not{\pi}$EFT-based on the generalization of nuclear cluster models is the so-called *halo/cluster* $\not{\pi}$EFT [91,92]. It was primarily introduced for investigating the clustering and halo phenomena in light nuclei with narrow resonances (often in higher partial waves), characterized by multi-scale threshold dynamics at energy scales often lower than that in standard $\not{\pi}$EFT. A *heteronuclear* subclass of systems often manifest themselves as exotic s-shell hypernuclei which typically lie along the limits of nuclear stability (so-called the drip-lines). These modified $\not{\pi}$EFTs exploit the separation of scales between the hard scale of the EFT and a hierarchy of dynamically generated low-energy scales associated with the formation of one or more shallow bound/resonance states. Such analysis has been successfully applied to study light hypernuclei, since the very first of such EFT work by Hammer [93] on the LO investigation of hypertriton ($^3_\Lambda$H), a Λnp Efimov-like bound system in the $I = 0, J = 1/2$ channel. Subsequently, a number of similar LO halo/cluster EFT works appeared in the literature, both in the $S = -1$ [94,95] and $S = -2$ [96–98] strangeness sectors, in the search for light exotic single and double Λ-hypernuclear states, e.g., $nn\Lambda$,[4] $^4_{\Lambda\Lambda}$He, $^5_{\Lambda\Lambda}$H, $^5_{\Lambda\Lambda}$He and $^6_{\Lambda\Lambda}$He. It is worth mentioning here that a novel ab initio LO $\not{\pi}$EFT technique using few-body stochastic variational method of calculation was suggested in

---

model-independent assessment which is beyond the scope of a simplistic qualitative treatment as pursued in this work.

---

[4] The $\not{\pi}$EFT analysis by Ando et al. [94] attempted to investigate the feasibility of the putative $nn\Lambda$ bound state, as reported by the HypHI Collaboration [99] in 2013. In that analysis a coupled system of integral equation was constructed in the physical basis involving only the spin projected couplings and excluding isospin projections for simplicity. This, however, yielded the asymptotic RG limit cycle scaling exponent as $s_0^{(nn\Lambda)} = 0.80339\ldots$, which is inconsistent with the expected universal scaling based on the the the relative three-particle mass ratios [68]. As recently elucidated by Hildenbrand and Hammer [95], the correct scaling could be achieved by a proper reformulation in the spin–isospin basis leading to the value, $s_0^{(nn\Lambda)} = 1.0076\ldots$. This value is identical to that obtained in the study of hypertriton, and also reproduces the well-known asymptotic scaling $s_0 = 1.00624\ldots$, for identical masses [68,90] (also see Appendix A.3). Furthermore, in Ref. [95] a threshold ground state appeared at the critical cut-off scale $\Lambda_{\text{reg}} \sim 600$ MeV, whereby the likelihood of a physically realizable Efimov-bound/resonance Λnn state may not be excluded outright. Notably, such a possibility had been completely ruled out earlier in Ref. [94] with the critical cut-off obtained as $\Lambda_{\text{reg}} \gtrsim 1.5$ GeV. Besides, it deserves mentioning here that nearly all potential model approaches till date have reported negative results for the existence of the Λnn bound state (see e.g., Refs. [100–103]). In particular, the Faddeev calculation analysis of Ref. [103] demonstrated using a complex scaling method that the strength of the Λn Yamaguchi-type (separable) potential is needed to be tuned $\sim 25\%$ above the realistic estimate in order for the Λnn system to emerge into a three-body bound state.

Refs. [104–107] for the study of ordinary nuclei on the lattice, the so-called *lattice nuclei*, facilitating easy comparison with results of Lattice QCD simulations at unphysical quark masses. Such a framework, which is complimentary to the halo $^{\#}$EFT approach, was later extended by Contessi et al. [108] in the $S = -1$ sector to seek a solution to the B_Λ-overbinding problem, and more recently in the feasibility studies of several light $S = -2$ double Λ-hypernuclei [109]. Here we re-emphasize that the above literature survey relating to studies on Λ-hypernuclei comprises only of noteworthy $^{\#}$EFT works motivated on the philosophy of few-body universality, as adopted in this paper. Needless to say, however, that the existing literature also includes an entire gamut of well acclaimed works based on ab initio and cluster potential models involving three- and four-body Faddeev–Yakubovsky and variational calculations (see, e.g., [3–6] and references therein). As these methodologies do not come under the direct purview of universal physics principles, a detailed discussion of the models, especially in the context of Λ-hypernuclear studies, is beyond the scope of this work.

3 Halo $^{\#}$EFT of $\Xi^- nn$

In this work, we use halo $^{\#}$EFT at LO to assess the feasibility of a $\Xi^- nn$ bound state in the $I = 3/2$, $J = 1/2$ channel primarily based of Efimov universality. This may be reflected through a study of the EFT regulator scale dependence of the RG limit cycle exhibited by the three-body contact interaction coupling (see Appendix A for basic details regarding few-body universality, RG limit cycle and Efimov effect in the context of EFT analysis). Despite existing uncertainties regarding the exact nature of ΞN interactions, we adopt a certain scenario motivated by the results from a series of recent constituent quark cluster potential model (CQCM) analyses [39,41–43] based on Faddeev calculations. These analyses rely on the fact that the $^3S_1$ $\Xi^- n$ sub-system is dominantly attractive and bound with large positive S-wave scattering length, namely, $a_{\Xi n}^{(j=1)} = 4.911$ fm, taken from the Nijmegen ESC08c model [60,61]. It is especially noted in some of these model studies that if one included the real bound $^3S_1$ channel as the only $\Xi^- n$ sub-system channel, the $\Xi^- nn$ system exhibited a three-body deeply bound state. On the other hand, no bound state is obtained with only the $^1S_0$ $\Xi^- n$ sub-system channel included with the Nijmegen model predicted small S-wave scattering length, namely, $a_{\Xi n}^{(j=0)} = 0.579$ fm [60,61].[5] Here we report analogous qualitative features arising in the context of our EFT framework as well. This probably hints at the consistency of our halo EFT results with those reported earlier in the above mentioned model

analyses. In particular, the Faddeev-type coupled integral equations in the momentum space are found not to exhibit an RG limit cycle with only the repulsive $^1S_0$ $\Xi^- n$ sub-system channel included, implying an unbound $\Xi^- nn$ system. On the other hand, we find that an asymptotic RG limit cycle (cf. Appendix A.3) is always manifest in the presence of the $\Xi^- n$ triplet channel, irrespective of the inclusion of the $\Xi^- n$ singlet channel. However, a full-fledged numerical evaluation of the integral equations using conventional auxiliary fields, or the so-called dibaryon formalism [72,73,82] (cf. Appendix A.1 for details), becomes a challenging task, especially when dealing with the repulsive $\Xi^- n$ sub-system with a small positive scattering length. The problem is attributed to the presence of a unphysically deep pole in the $^1S_0$ $\Xi^- n$ dibaryon propagator [cf. Eq. (8)] corresponding to an unnaturally large binding momentum, $\gamma_{\Xi n}^{(0)} \approx 1/a_{\Xi n}^{(0)} \approx 340$ MeV (estimated using the the Nijmegen ESC08c model [60,61]). Since there is no straightforward way of "renormalizing" the effect of such a deep two-body pole, the EFT evidently breaks down. Thus, in this work we take recourse to a simplistic study of the $\Xi^- nn$ system to look for possible emergence of physically realizable Efimov-like trimers by completely excluding the repulsive $^1S_0$ $\Xi^- n$ channel (as done in e.g., Ref. [39]). Notably, in our halo EFT formalism, the triplet dibaryon pole position defines the $n + (\Xi^- n)_t$ particle-triplet-dimer break-up threshold, beyond which the $\Xi^- nn$ trimer levels are expected to emerge. The trimer binding energies correspond to the eigensolutions to the coupled integral equations for a given finite value of an ultraviolet (UV) sharp momentum cut-off regulator [68] (cf. Appendix A.2).

In the ensuing EFT analysis, we present a qualitative investigation of the regulator scale dependence of an a priori undetermined three-body contact interaction coupling introduced for the purpose of renormalization. Through this study, we hope to establish a correspondence between our EFT results with those obtained in the potential model analyses by Garcilazo et al. [39,41–43]. Our analysis serves as a consistency check between both types of approaches. In particular, based on existing model estimates for the three-body binding energy, we give a naive window of possible estimates of the S-wave three-body scattering length associated with the elastic $n - (\Xi^- n)_t$ scattering process. These predictions in turn induce a striking feature of three-body universality, the so-called Phillips line [111], namely, the fact that different model potentials tuned to the same input two-body scattering data (i.e., $a_{\Xi n}^{(j=1)}$ and a_{nn}) yield a highly correlation result for the $\Xi^- nn$ binding energy and the corresponding three-body scattering length. Albeit approximations considered in our simplistic model-independent treatment, such universal correlations are expected to reflect robust features of the thee-body system.

---

[5] It is notable that the $^1S_0$ nn sub-system channel is virtual bound with large negative S-wave scattering length, namely, $a_{nn} = -18.63$ fm [110].

3.1 Effective Lagrangian and formalism

In a simplified picture, the Ξ^-nn system may be visualized as a two-neutron halo with the two loosely bound neutrons orbiting about the Ξ^--hyperon "elementary" core, forming a shallow bound state with a diffuse structure. Such universal class of systems exploits the distinct separation of scale between the typical dynamical scale, $Q \sim \gamma_{\Xi n}^{(1)} \approx 1/a_{\Xi n}^{(1)} \sim 40$ MeV, associated with the "attractive pole" momentum of the $^3S_1$ Ξ^-n dibaryon propagator (ignoring possible artifact due to the deep pole at $\gamma_{\Xi n}^{(0)} \approx 1/a_{\Xi n}^{(0)} \sim 340$ MeV associated with the repulsive $^1S_0$ Ξ^-n sub-system), and the breakdown scale $\Lambda_H \sim m_\pi$ of standard $\not\pi$EFT [68,72–83]. This implies that $\epsilon \sim Q/m_\pi \sim 1/3$ defines a reasonable expansion parameter that is amenable to a EFT treatment. A concise description on the general principles and methodology of $\not\pi$EFT framework used in the analyses of two- and three-body universality is provided in Appendix A. The effective Lagrangian is constructed on the basis of all possible available low-energy symmetries ($\mathcal{P}$, $\mathcal{C}$, $\mathcal{T}$ and Galilean invariance) and degrees of freedom. The interaction vertices are represented by local contact interactions and the Lagrangian is expressed in a derivative expansion of the fundamental fields. For our system, the fundamental degrees of freedom consist of the Ξ^--hyperon and neutron (n) fields. The LO non-relativistic Lagrangian is free from derivative terms and expressed as a sum of one-, two- and three-body parts, namely,

$$\mathcal{L}_{\not\pi\text{EFT}} = \mathcal{L}_{1-\text{body}} + \mathcal{L}_{2-\text{body}} + \mathcal{L}_{3-\text{body}}. \qquad (1)$$

Below we consider each of the components of the effective Lagrangian separately.

One-body part. The terms $\mathcal{L}_\Xi$ and $\mathcal{L}_n$ constitute the one-body Lagrangian $\mathcal{L}_{1-\text{body}}$ corresponding to the kinetic part of the Ξ^--hyperon and neutron fields, respectively, and are expressed in the physical basis as

$$\mathcal{L}_{1-\text{body}} = \mathcal{L}_\Xi + \mathcal{L}_n , \qquad (2)$$

where

$$\mathcal{L}_\Xi = \Xi^\dagger \left[iv \cdot \partial + \frac{(v \cdot \partial)^2 - \partial^2}{2M_\Xi} \right] \Xi ,$$

$$\mathcal{L}_n = n^\dagger \left[iv \cdot \partial + \frac{(v \cdot \partial)^2 - \partial^2}{2M_n} \right] n , \qquad (3)$$

where M_Ξ and M_n are the physical masses of the Ξ^--hyperon and neutron fields respectively, as given in Table 1, and $v^\mu = (1, \mathbf{0})$ is the four-velocity vector which is used to express the Lagrangian in a manifestly covariant manner akin to the heavy-baryon formalism [113]. It follows that the non-relativistic propagators associated with these fundamental fields are given by

$$iS_\Xi(p_0, \mathbf{p}) = \frac{i}{p_0 - \frac{\mathbf{p}^2}{2M_\Xi} + i\eta} ,$$

Table 1 PDG [112] values of particle masses considered in the analysis

Particle	Mass symbol	Numerical value (MeV)
Ξ-Hyperon	M_Ξ	1321.710
Neutron (n)	M_n	939.565

$$iS_n(p_0, \mathbf{p}) = \frac{i}{p_0 - \frac{\mathbf{p}^2}{2M_n} + i\eta} ; \quad \eta \to 0 , \qquad (4)$$

where p_0 and $\mathbf{p}$ are temporal and spatial parts of the generic four-momentum p^μ.

Two-body part. In $\not\pi$EFT, to deal with the formation of shallow S-wave bound states one needs to *unitarize* the two-body sector by employing the so-called Kaplan-Savage-Wise (KSW) power counting rule [76–80]. To efficiently capture such two-body physics in the vicinity of a *non-trivial fixed-point* described by the RG of the two-body contact interactions, it was suggested to introduce auxiliary *dimer* fields in the effective Lagrangian [68,72,73,81,82] (also, see Appendix A.1). Thus, for the heteronuclear Ξ^-nn system we need to introduce two types of dimer fields, namely, the isospin-spin triplet $(i = 1, j = 1)$ Ξ^-n dibaryon field u_1 and the isospin-triplet spin-singlet $(i = 1, j = 0)$ nn dibaryon field u_0. Here we re-emphasize that the iso-triplet spin-singlet $(i = 1, j = 0)$ Ξ^-n sub-system channel is considered decoupled from the picture as its physics lies beyond the realm of our halo EFT formalism. The corresponding two-body LO Lagrangian (written in the physical basis) in terms of the dibaryon fields is expressed as

$$\mathcal{L}_{2-\text{body}} = \mathcal{L}_{u_0} + \mathcal{L}_{u_1} , \qquad (5)$$

where

$$\mathcal{L}_{u_0} = -(u_0)^{a\dagger} \left[iv \cdot \partial + \frac{(v \cdot \partial)^2 - \partial^2}{4M_n} \right] (u_0)^a$$
$$- y_0 \left[(u_0)^{a\dagger} \left(n^T \hat{\mathscr{P}}_{(nn)}^{(1,0)\,a} n \right) + \text{h.c.} \right] ,$$

$$\mathcal{L}_{u_1} = -(\mathbf{u}_1)_k^{a\dagger} \left[iv \cdot \partial + \frac{(v \cdot \partial)^2 - \partial^2}{2(M_\Xi + M_n)} \right] (\mathbf{u}_1)_k^a$$
$$- y_1 \left[(\mathbf{u}_1)_k^{a\dagger} \left(n^T \hat{\mathscr{P}}_{(\Xi n)\,k}^{(1,1)\,a} \Xi \right) + \text{h.c.} \right] ,$$

$$(6)$$

noting that the "wrong signs" in front of the respective kinetic terms suggest the non-dynamical or quasi-particle nature of the dibaryon fields. Here, $\hat{\mathscr{P}}_{(\Xi n)\,k}^{(1,1)\,a} = \frac{1}{2}\tau^2\tau^a\sigma_2\sigma_k$, and $\hat{\mathscr{P}}_{(nn)}^{(1,0)\,a} = \frac{1}{\sqrt{8}}\tau^2\tau^a\sigma_2$ are the spin–isospin projection operators, with σ_k and τ^a $(k, a = 1, 2, 3)$ being the Pauli matrices in the spin and isospin spaces respectively. The two-body non-derivatively coupled LO contact interactions or LECs $y_{0,1}$ between the respective dibaryons and their constituent elementary

fields encode all UV physics that remain unresolved in the EFT. These couplings are easily fixed by the prescription given in Ref. [114]:

$$y_1 = \sqrt{\frac{2\pi}{\mu}}, \quad \text{and} \quad y_0 = \sqrt{\frac{4\pi}{M_n}}, \qquad (7)$$

where $\mu = M_n M_\Xi/(M_n + M_\Xi) = 549.174$ MeV is the reduced mass of $\Xi^- n$ two-body sub-system. Next, we spell out the renormalized "dressed" (unitarized) propagators for the nn and $\Xi^- n$ dibaryon fields (cf. Fig. 1) consistent with the KSW power counting scheme [76–80]:

$$i\mathscr{D}_0(p_0,\mathbf{p}) = \frac{4\pi}{y_0^2 M_n} \frac{i}{\gamma_{nn}^{(0)} - \sqrt{-M_n(p_0 - \frac{\mathbf{p}^2}{4M_n}) - i\eta} - i\eta},$$

$$i\mathscr{D}_1(p_0,\mathbf{p}) = \frac{2\pi}{y_1^2 \mu} \frac{i}{\gamma_{\Xi n}^{(1)} - \sqrt{-2\mu(p_0 - \frac{\mathbf{p}^2}{2(M_n+M_\Xi)}) - i\eta} - i\eta};$$

$$\eta \to 0, \qquad (8)$$

where at the LO in $\not\!\pi$EFT, we have $\gamma_{nn}^{(0)} \to 1/a_{nn}$ and $\gamma_{\Xi n}^{(1)} \to 1/a_{\Xi n}^{(1)}$, as the (1,0) nn and (1,1) $\Xi^- n$ dibaryon (virtual or real bound) binding momenta, respectively. It may be noted that the two scattering lengths are the only two-body input parameters in our LO EFT. Other parameters, such as S-wave effective range r_{nn} and $r_{\Xi n}$ formally contribute at NLO in the KSW power counting scheme, which is beyond the scope of this work.

Three-body part. Formally the $\Xi^- nn$ three-body system with a possible fine-tuned two-body sector exhibits the well-known Efimov effect close to the unitary or resonant limit of the two-body interactions. This is reflected by the fact that the integral equations for the system with only two-body contact interactions become ill-defined in the asymptotic UV limit. The inherent reason for this anomalous UV behavior is the partial breakdown of the expected *fixed-point scaling* invariance of the system in the vicinity of bound states into the onset of a *discrete scaling* symmetry. A possible remedy to this problem, for instance, may be obtained by including a sharp momentum UV cut-off regulator Λ_{reg} in the integral equations, thereby, formally introducing another free parameter in the LO EFT (in addition to the two S-wave scattering lengths in the two-body sector). This simultaneously necessitates the introduction of LO three-body contact interactions (3BFs) as counterterms with scale dependent couplings, such as $g_3(\Lambda_{\text{reg}})$, to renormalize the artificial cut-off dependence. The resulting atypical scaling behavior gets reflected through the emergence of a RG limit cycle behavior in the 3BF couplings (for a pedagogical review on this topic, see Ref. [68]; also see Appendices A.2 and A.3). Here we present a certain choice of the LO three-body Lagrangian consistent with the reparametrization symmetries of the coupled system of integral equation, and given by

$$\mathcal{L}_{3-\text{body}} = -\frac{g_3(\Lambda_{\text{reg}})}{\Lambda_{\text{reg}}^2}\left[\frac{M_\Xi y_1^2}{2}\left\{(\mathbf{u}_1)_l^a \, \hat{\mathcal{P}}_l^{ab} \, n\right\}^\dagger \right.$$
$$\times \left\{(\mathbf{u}_1)_k^c \, \hat{\mathcal{P}}_k^{cb} \, n\right\}$$
$$\left. -\frac{\sqrt{3}M_n y_0 y_1}{\sqrt{2}}\left\{(\mathbf{u}_1)_l^a \, \hat{\mathcal{P}}_l^{ab} \, n\right\}^\dagger\left\{u_0^c \, \hat{\mathcal{P}}^{cb} \, \Xi\right\} + \text{h.c.}\right], \qquad (9)$$

where the spin–isospin projection operators have the following forms:

$$\left[\hat{\mathcal{P}}_k^{cb}\right]_{\alpha\beta} = \frac{1}{3\sqrt{3}}\left[(\tau^c\tau^b)_{\alpha\beta} + \delta_{cb}\delta_{\alpha\beta}\right]\sigma_k,$$
$$\left[\hat{\mathcal{P}}^{cb}\right]_{\alpha\beta} = \frac{1}{3}\left[(\tau^c\tau^b)_{\alpha\beta} + \delta_{cb}\delta_{\alpha\beta}\right], \qquad (10)$$

with $\alpha,\beta = 1,2$ being the isospin-1/2 SU(2) indices [115]. The cut-off dependence of g_3 is *a priori* undetermined in the EFT and can be fixed only using a three-body datum, e.g., the three-body binding energy B_3 or the corresponding scattering length a_3.[6] However, none of these empirical information is available currently, either from experimental data or from *ab initio* lattice QCD simulations. Due to such acute paucity of data, it becomes imperative to rely on some of the erstwhile phenomenological models, before our LO EFT analysis can be made viable to yield some qualitative insight. Thus, for example, here we rely on the $\Xi^- nn$ binding energy estimates from the Faddeev calculations provided by the potential model analyses of Refs. [38,39,41–43].

3.2 Coupled STM integral equations

For the sake of theoretical analysis, we study the $\Xi^- nn$ system in both the kinematical three-body bound and scattering domains. For this purpose, we choose a representative elastic reaction channel corresponding to the low-energy $1 + 2 \to 1 + 2$ scattering process with dominant S-wave contribution, namely,

$$n + (\Xi^- n)_t \longrightarrow n + (\Xi^- n)_t. \qquad (11)$$

Here we must emphasize that this "reference" scattering process is chosen solely for demonstrating our theoretical methodology, irrespective of the infeasibility of performing such experiments at current facilities. The chosen reaction channel yields a set of two coupled Fredholm-type integral equations in the momentum space. While their eigenvalues yield all possible allowed

---

[6] The three-body datum in this case is analogous to the information on parameters, such as Λ_* or κ_*, in addition to the two-body scattering length a_0, necessary for the description of the Efimov spectrum, as detailed in Appendix A.3 for a three-boson system.
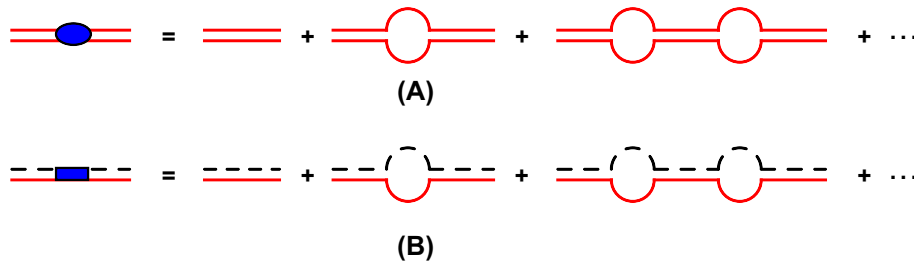
Eur. Phys. J. Spec. Top. (2021) 230:579–601

585

Fig. 1 The renormalized dressed propagators for (upper panel) $^3S_1$ nn, and (lower panel) $^3S_1$ $\Xi^- n$ dibaryon fields. The dashed lines represent the Ξ^--hyperon field propagator and the solid lines represent the neutron field propagator
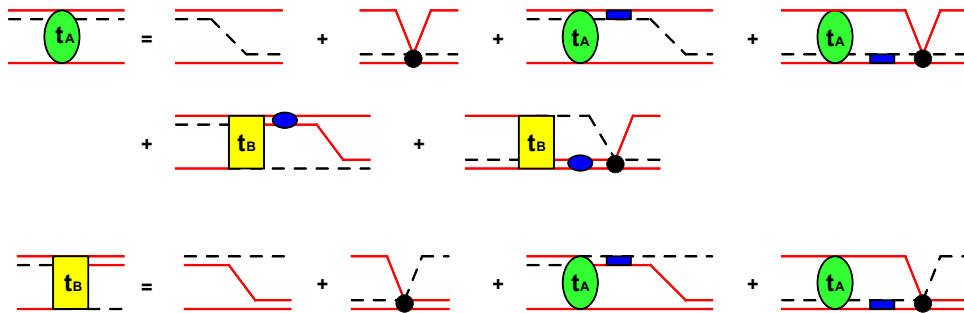

Fig. 2 Feynman diagrams for the representative coupled channel elastic scattering process, $n+(\Xi^- n)_t \to n+(\Xi^- n)_t$, where "$t$" is used to denotes the $^3S_1$ $\Xi^- n$ sub-system. The solid (dash) line represents neutron (Ξ^--hyperon) propagator. The off-shell double lines with insertions of the small empty oval (square) blobs represent the renormalized

dressed $^1S_0$ nn (u_0) and $^3S_1$ $\Xi^- n$ (u_1) dibaryon field propagators. The large blob t_A (t_B) denotes the elastic (inelastic) half-off-shell scattering amplitude for the $n + u_1 \to n + u_1$ ($n + u_1 \to \Xi^- + u_0$) scattering processes. The dark blobs represent the insertion of leading order three-body contact interactions

trimer binding energies (B_3), the eigenvectors yield the scattering amplitudes of the coupled elastic and inelastic channels. In Fig. 2, we display the relevant Feynman diagrams for the above mentioned scattering process expressed in term of the two *half-off-shell* S-wave projected scattering amplitudes, namely, $t_A(k, p; E)$ representing the elastic process $n+u_1 \to n+u_1$, and $t_B(k, p)$ representing the inelastic process $n + u_1 \to \Xi^- + u_0$. Here $k = |\mathbf{k}|$ ($p = |\mathbf{p}|$) denotes the on-shell (off-shell) incoming (outgoing) relative three-momentum in the center-of-mass (CM) system, and E is the total CM kinetic energy of the three-body system, given by

$$E = \pm \frac{k^2}{2\mu_{n(n\Xi)}} - \mathcal{B}_2; \quad \mathcal{B}_2 = \frac{\left(\gamma_{\Xi n}^{(1)}\right)^2}{2\mu} = 1.47 \text{ MeV},$$
(12)

vspace*-8pt where the "−" sign is applicable for the kinematical three-body bound state domain and the "+" sign for the scattering domain. $\mathcal{B}_2$ is the CM binding energy of a possible shallow-bound $(\Xi^- n)_t$ sub-system which also sets the scale for the particle-triplet-dimer ($n + u_1$) break-up threshold energy,[7] and $\mu_{n(n\Xi)} = M_n(M_\Xi + M_n)/(2M_n + M_\Xi) = 663.768 \text{ MeV}$

---

[7] In our halo EFT formalism $\mathcal{B}_2$ corresponds to the pole position of the u_1 dibaryon propagator. Its value may be compared with the binding energy of the putative D^* state in the (1,1) ΞN channel, as predicted by the potential model analyses of Refs. [42,43,60,61].

is the corresponding reduced mass of three-body (particle-dimer) system. The construction methodology of the integral equations is similar to those employed in several earlier ${}^{\#}$EFT works [67,94,96–98] (also see Appendix B). The renormalized S-wave projected coupled (elastic and inelastic channels) STM integral equations with the introduced cut-off regulator Λ_{reg} are given as

$$t_A^{(R)}(p, k; E) = \mathcal{Z}_{\Xi n} \frac{(y_1^2 M_\Xi)}{2} \left[K_{(a)}(p, k; E) - \frac{g_3(\Lambda_{\text{reg}})}{\Lambda_{\text{reg}}^2} \right]$$
$$- \frac{M_\Xi}{2\pi\mu} \int_0^{\Lambda_{\text{reg}}} dq\, q^2 \left[K_{(a)}(p, q; E) - \frac{g_3(\Lambda_{\text{reg}})}{\Lambda_{\text{reg}}^2} \right]$$
$$\times \mathcal{D}_1 \left(E - \frac{q^2}{2M_n}, \mathbf{q} \right) t_A^{(R)}(q, k; E)$$
$$+ \frac{\sqrt{6}y_1}{\pi y_0} \int_0^{\Lambda_{\text{reg}}} dq\, q^2 \left[K_{(b2)}(p, q; E) - \frac{g_3(\Lambda_{\text{reg}})}{\Lambda_{\text{reg}}^2} \right]$$
$$\times \mathcal{D}_0 \left(E - \frac{q^2}{2M_\Xi}, \mathbf{q} \right) t_B^{(R)}(q, k; E),$$
(13)

and

$$t_B^{(R)}(p, k; E) = -\mathcal{Z}_{\Xi n} \sqrt{\frac{3}{2}} (y_1 y_0 M_n) \left[K_{(b1)}(p, k; E) - \frac{g_3(\Lambda_{\text{reg}})}{\Lambda_{\text{reg}}^2} \right]$$
$$+ \sqrt{\frac{3}{2}} \frac{M_n y_0}{\mu\pi y_1} \int_0^{\Lambda_{\text{reg}}} dq\, q^2 \left[K_{(b1)}(p, q; E) - \frac{g_3(\Lambda_{\text{reg}})}{\Lambda_{\text{reg}}^2} \right]$$
$$\times \mathcal{D}_1 \left(E - \frac{q^2}{2M_n}, \mathbf{q} \right) t_A^{(R)}(q, k; E),$$
(14)

586

Eur. Phys. J. Spec. Top. (2021) 230:579–601

where the term $K_{(a)}$ denotes the S-wave projected Ξ-exchange interaction kernel, while $K_{(b_1,b_2)}$ are two variants of the n-exchange interaction kernel, namely,

$$K_{(a)}(p,\kappa;E) = \frac{1}{2p\kappa} \ln\left(\frac{p^2+\kappa^2+ap\kappa-2\mu E}{p^2+\kappa^2-ap\kappa-2\mu E}\right),$$

$$K_{(b_1)}(p,\kappa;E) = \frac{1}{2p\kappa} \ln\left(\frac{bp^2+\kappa^2+p\kappa-M_nE}{bp^2+\kappa^2-p\kappa-M_nE}\right),$$

$$K_{(b_2)}(p,\kappa;E) = \frac{1}{2p\kappa} \ln\left(\frac{p^2+b\kappa^2+p\kappa-M_nE}{p^2+b\kappa^2-p\kappa-M_nE}\right).$$

$$(15)$$

The generic momentum κ denotes either the incoming on-shell relative momentum (k) or the loop momentum (q). Also, $a = 2\mu/M_\Xi$ and $b = M_n/(2\mu)$ are two mass-dependent parameters. The above half-off-shell renormalized amplitudes are related to the corresponding unrenormalized amplitudes $t_{A,B}(p,k;E)$ by

$$t_{A,B}^{(R)}(p,k;E) = \sqrt{\mathcal{Z}_{\Xi n}}\, t_{A,B}(p,k;E)\, \sqrt{\mathcal{Z}_{\Xi n}}, \quad (16)$$

where

$$\mathcal{Z}_{\Xi n}^{-1} = \frac{y_1^2 \mu^2}{2\pi \gamma_{\Xi n}^{(1)}}, \quad (17)$$

is the wavefunction renormalization associated with the possible bound $(\Xi^- n)_t$ sub-system. Finally, the renormalized elastic amplitude is used to obtain the S-wave $n-(\Xi^- n)_t$ three-body scattering length by considering the threshold limit of the on-shell momentum $k \to 0$, namely,

$$a_3 = -\lim_{k\to 0} \frac{\mu_{n(n\Xi)}}{2\pi}\, t_A^{(R)}(k,k). \quad (18)$$

3.3 Asymptotic analysis

To assess that the coupled STM integral equations indeed have the potentiality to yield three-body bound state solutions, one needs to check for possible manifestation of Efimov effect at the asymptotic UV limit as $\Lambda_{\text{reg}} \to \infty$ [68] (cf. Appendix A.3). In this case, all other low-energy/momentum scales in the problem, e.g., $E, \gamma_{\Xi n}^{(1)}, \gamma_{nn}^{(0)}, k \ll p, q \sim \Lambda_{\text{reg}} \lesssim \infty$, become irrelevant, and the integral equations can be well approximated by considering only the homogeneous parts (i.e., excluding the tree diagram contributions in Fig. 2) and dropping all the k dependence and three-body interactions (g_3) terms. Thus, with no other relevant scales in the theory, the STM equations become *dilation* invariant and symmetric under the inversion transformation $q \to 1/q$. Consequently, the half-off-shell channel amplitudes exhibit a power-law scaling, namely, $t_{A,B}(\kappa) \sim \kappa^{s-1}$, with $\kappa \sim \Lambda_{\text{reg}}$ and a complex-valued exponent s, an undetermined three-body parameter. By performing a sequence of *Mellin* transformations the integral equations can be converted into a single transcendental equation which solves for the exponent s, namely,

$$1 = \frac{M_\Xi}{2\mu C_1}\left[\frac{\sin[s\sin^{-1}(a/2)]}{s\cos(\pi s/2)}\right]$$
$$+ \frac{3M_n}{\mu C_1 C_2}\left[\frac{\sin[s\cot^{-1}\sqrt{4b-1}]}{s\cos(\pi s/2)}\right]^2,$$

$$(19)$$

where

$$C_1 = \sqrt{\frac{\mu}{\mu_{n(n\Xi)}}}, \quad \text{and} \quad C_2 = \sqrt{\frac{M_n}{2\mu_{\Xi(nn)}}}, \quad (20)$$

and $\mu_{\Xi(nn)} = 2M_n M_\Xi/(2M_n + M_\Xi) = 775.942$ MeV is the reduced mass of the $\Xi^- + u_0$ particle-dimer system. Solving Eq. (19) yields an imaginary solution, i.e., $s = \pm i s_0^\infty = \pm i 0.803391\ldots$. The solution immediately suggests the existence of an asymptotic UV RG limit cycle with a discrete scaling symmetry associated with the scale factor, $\lambda_\infty = e^{\pi/s_0^\infty} = 49.919712\ldots$. This formally implies that our LO EFT manifests Efimov effect in the unitary limit of the $\Xi^- nn$ system. Consequently, it becomes imperative to include scale-dependent 3BF as counterterms in the effective Lagrangian to renormalize the ill-defined asymptotic limit of the STM equations with two-body interaction. As elucidated by power counting arguments in the Appendix A.2, such non-derivative 3BF terms are naturally enhanced to get promoted to LO for consistency of the renormalization scheme [72,73]. Here we must, however, mention that the asymptotic scaling exponent $s_0^\infty = 0.803391\ldots$ considerably differs from the expected value, $(s_0^\infty)_{\text{expect}} \sim 1.01$, based on the universal RG limit cycle scaling depending on the relative three-particle mass ratios [68]. This difference is attributed to the effect of excluding the isospin-triplet spin-singlet $(1,0)$ $\Xi^- n$ sub-system channel from the STM equations whose dynamics are not directly amenable to our low-energy EFT description.

4 Results and discussion

In this section, we present the results of our preliminary investigation of the sharp cut-off regulator (Λ_{reg}) dependence of the Faddeev-type STM integral Eqs. (13) and (14), at non-asymptotic low-energy scales. For the sake of numerical evaluations, we use the particle masses as presented in Table 1, while the S-wave scattering lengths $a_{nn} = -18.63$ fm [110] and $a_{\Xi n}^{(j=1)} = 4.911$ fm [60,61] constitute the principal input two-body parameters in our LO EFT framework. In the last section, our asymptotic analysis demonstrated the evidence of Efimov effect at the unitary limit of the $\Xi^- nn$ system with an RG limit cycle discrete scal-
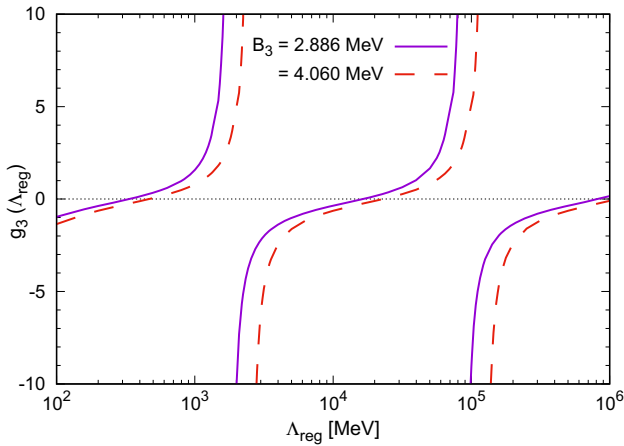
Fig. 3 The approximate RG limit cycle behavior of the three-body coupling g_3 for the $\Xi^- nn$ ($I = 3/2$, $J = 1/2$) system as a function of the cut-off scale Λ_{reg}. The results are obtained by numerically solving the STM integral Eqs. (13) and (14). The input three-body binding energies $B_3 = 2.886$, 4.06 MeV, are predictions from the Faddeev calculation based potential models [39,43]. The input S-wave spin–isospin triplet $\Xi^- n$ scattering length $a_{\Xi n}^{(j=1)} = 4.911$ fm is provided by the recently updated ESC08c Nijmegen potential model analyses [60,61]

ing symmetry determined by the multiplicative factor $\lambda_\infty = e^{\pi/s_0^\infty} \sim 50$. With $\kappa^{(1)} \equiv \gamma_{\Xi n}^{(1)} \sim 40$ MeV as the typical momentum scale of the problem, it is natural to expect that the next higher momentum scale appears at $\kappa^{(2)} \equiv \lambda_\infty \gamma_{\Xi n}^{(1)} \sim 2$ GeV $\gg \Lambda_H \sim m_\pi$, which is well beyond the accessibility of our low-energy EFT description. Hence, it is likely that at the most one Efimov-like state emerges as a plausible bound $\Xi^- nn$ hypernucleus, if at all. Figure 3 shows the cut-off dependence of the three-body contact interaction coupling $g_3(\Lambda_{\mathrm{reg}})$. In the absence of datum to constrain the unknown coupling g_3, our *strategy* is to hypothetically assume at the very outset that the $\Xi^- nn$ system is bound, with ground state eigenenergy ($E = -B_3$) coinciding with the existing (Faddeev calculations) model predictions of Refs. [39,41–43]. We thereby fix our benchmark range of input values of the $\Xi^- nn$ binding energy, namely, between $B_3 = 2.886$ MeV taken from Ref. [43] and $B_3 = 4.06$ MeV taken from Ref. [39]. Notably, both predictions rely on the same two-body input parameters (e.g., $a_{\Xi n}^{(1)} = 4.911$ fm) provided by the recent ESC08c Nijmegen model analyses [60,61].[8] The figure displays the typical quasi-periodic log-singularities of *approximate* RG limit cycles for the two aforementioned

---

[8] The predicted value $B_3 = 2.886$ MeV obtained in Faddeev calculation analysis of Ref. [43] resulted from considering both the repulsive (1,0) and attractive (1,1) ΞN channels, whereas the value $B_3 = 4.06$ MeV obtained in the Faddeev analysis of Ref. [39] resulted from considering only the latter attractive channel. Nevertheless, irrespective of these details, we consider these predicted values as given three-body inputs to our EFT analysis.

limiting B_3 inputs. The corresponding non-asymptotic scale factor, $\lambda_n \lesssim \lambda_\infty$, may be obtained by considering the ratio of two successive cut-offs where the three-body coupling vanishes, i.e., if $g_3\left(\Lambda_{\mathrm{reg}}^{(n)}\right) = g_3\left(\Lambda_{\mathrm{reg}}^{(n+1)}\right) = 0$, then

$$\lambda_n = \frac{\Lambda_{\mathrm{reg}}^{(n+1)}}{\Lambda_{\mathrm{reg}}^{(n)}} \; ; \quad n = 1, 2, \ldots, \infty , \qquad (21)$$

where $\Lambda_{\mathrm{reg}}^{(n)}$ is the cut-off corresponding to n^{th} zero of g_3. Table 2 displays some of the estimated non-asymptotic scale factors λ_n corresponding to successive pairs of zeros of each RG limit cycle obtained for the two limiting input B_3 values. In each case, the scale factor λ_n is obtained close to yet less than the asymptotic value λ_∞. By progressively choosing larger pairs of the successive zeros of g_3, i.e., with $n \to \infty$, λ_n is found to converge rapidly to λ_∞.

Next, in Fig. 4 we display the cut-off variation of the binding energy B_3 excluding the 3BF terms, i.e., with $g_3 = 0$ in the STM equations. In particular, due to the ambiguities concerning the precise nature of the (1,1) ΞN sub-system interactions between different existing phenomenological analyses [34,44,49–61], we consider here two representative scenarios with contrasting perspectives as elucidated below (both cases can formally lead to the emergence of Efimov-like states):

– First, the scenario with the input positive $(\Xi^- n)_t$ scattering length, e.g., $a_{\Xi n}^{(j=1)} = 4.911$ fm, as predicted by the updated ESC08c Nijmegen potential model analyses [60,61], suggests a strongly attractive $^3S_1$ $\Xi^- n$ sub-system commensurate with the likely existence of a threshold bound state (D^*) [42,43]. Consequently, in the three-body sector with a pair of likely bound $(\Xi^- n)_t$ sub-systems and a virtual bound nn sub-system, the $\Xi^- nn$ system assumes a halo-bound samba-configuration [116] structure emerging from the particle-triplet-dimer $(n + (\Xi^- n)_t)$ break-up threshold at the CM energy $E = -\mathcal{B}_2$. This corresponds to the solid (red) line curve in the left panel of Fig. 4, representing the regulator dependence of the *relative* binding energy $B_d = B_3 - \mathcal{B}_2$, for the ground ($n = 0$) Efimov-like state which appears at the *critical cut-off* scale $\Lambda_{\mathrm{crit}}^{(0)} \approx 80$ MeV.
– Second, the scenario with the input negative $(\Xi^- n)_t$ scattering length, e.g., as predicted by the two recent SU(3) chiral EFT analyses, namely, $a_{\Xi n}^{(j=1)} = -0.09$ fm [56] and -1.17 fm [57], suggests a weakly attractive $^3S_1$ $\Xi^- n$ sub-system that is unlikely to exhibit any two-body bound state. Consequently, in the three-body sector with no bound two-body sub-systems, the $\Xi^- nn$ system assumes a bound Borromean-configuration [116] structure emerging from the three-particle break-up threshold $E = 0$. This corresponds to the two broken line curves in the right panel of Fig. 4, representing the regulator

588

Eur. Phys. J. Spec. Top. (2021) 230:579–601

Table 2 The approximate RG limit cycle behavior with the discrete scaling symmetry factor $\lambda_n \to \lambda_\infty$, obtained by solving the integral Eqs. (13) and (14) for the $\Xi^- nn$ ($I = 3/2$, $J = 1/2$) system

Binding energy B_3 (MeV)	$n \in \mathbb{Z}_+$	n^{th} zero of g_3 $\Lambda_{\text{reg}}^{(n)}$ (MeV)	$(n+1)^{\text{th}}$ zero of g_3 $\Lambda_{\text{reg}}^{(n+1)}$ (MeV)	Scale factor $\lambda_n = \Lambda^{(n+1)}/\Lambda^{(n)}$
2.886 [43]	1	334.283	16344.134	48.893105...
	2	16344.134	815412.631	49.890232...
	3	815412.631	40704680.527	49.919119...
	4	40704680.527	2031965537.021	49.919702...
4.06 [39]	1	465.937	22919.007	49.189069...
	2	22919.007	1143628.429	49.898690...
	3	1143628.429	57089119.370	49.919290...
	4	57089119.370	2849872042.899	49.919706...

Here, results for $n \leq 4$ display a rapid convergence of the scale parameter toward the asymptotic limit, $\lambda_\infty = 49.919712\ldots$. The input three-body binding energies $B_3 = 2.886$, 4.06 MeV are predictions from the Faddeev calculation-based potential models [39,43] with input S-wave $\Xi^- n$ ${}^3S_1$ scattering length $a_{\Xi n}^{(1)} = 4.911$ fm, provided by the ESC08c Nijmegen potential model analyses [60,61]
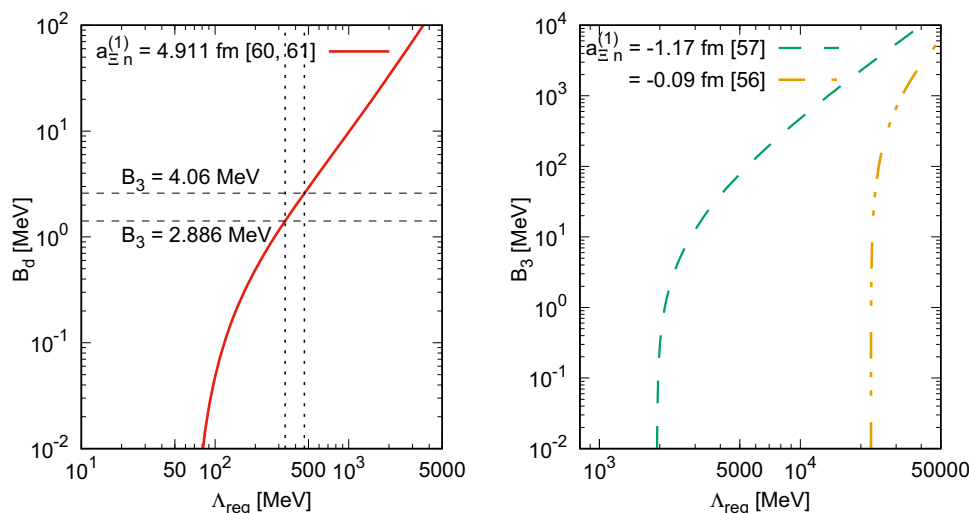

Fig. 4 Cut-off regulator (Λ_{reg}) dependence of the three-body binding energy of the $\Xi^- nn$ ($I = 3/2$, $J = 1/2$) system, obtained by solving the coupled integral Eqs. (13) and (14), excluding the three-body contact interactions [i.e., $g_3(\Lambda_{reg}) = 0$]. Left panel: Three-body binding energy $B_d = B_3 - \mathcal{B}_2$, relative to the $n + (\Xi^- n)_t$ particle-dimer threshold $-E = \mathcal{B}_2 = 1.47$ MeV, with the input S-wave ${}^3S_1$ $\Xi^- n$ scattering length $a_{\Xi n}^{(1)} = 4.911$ fm, as predicted by the recently updated ESC08c Nijmegen potential model analyses [60,61]. The regulator independent predictions, namely, $B_3 = 2.886$ MeV and 4.06 MeV, from the Faddeev calculation-based potential model analyses [39,43] for the same $a_{\Xi n}^{(j=1)}$ input are displayed for comparison. Right panel: Three-body binding energy B_3 relative to the three-particle threshold with input $a_{\Xi n}^{(j=1)} = -0.09, -1.17$ fm, as predicted by the two recent SU(3) chiral EFT analyses [56,57]

dependence of B_3 for the respective ground Efimov-like states which appear above the threshold at the critical values, $\Lambda_{\text{crit}}^{(0)} \approx 1940$ MeV for Ref. [57] and 22470 MeV for Ref. [56].

Evidently, with such large critical cut-offs, the latter scenario most likely not be supported in our low-energy EFT framework, *vis-a-vis*, the Efimov-like ground state does not physically manifest as a bound Ξ-hypernucleus. In contrast, the small critical cut-off in the former scenario lies well within the EFT validity domain, indicating an encouraging prospect for a poten-

tially feasible $\Xi^- nn$ Efimov state. In what follows, we shall only discuss our results pertaining to the former choice of the $\Xi^- nn$ scenario.

In the absence of the three-body contact interactions for renormalization, our results for the three-body binding energy exhibit considerable sensitivity to the cut-off variations. Figure 4 also compares our results with the regulator independent predictions for the $\Xi^- nn$ binding energy from the potential models [39,43] which also rely on the two-body inputs from the Nijmegen ESC08c model analyses [60,61]. We find that our scale-dependent eigenenergies from the STM equations reproduce the model predictions, namely, $B_3 = 2.886$ MeV
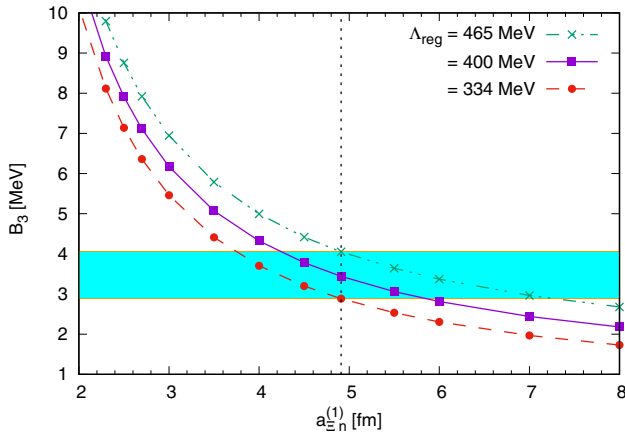
Fig. 5 Variation of the three-body binding energy B_3 of the $\Xi^- nn$ ($I = 3/2$, $J = 1/2$) system as a function of input positive values of the S-wave $^3S_1$ $\Xi^- n$ scattering length $a_{\Xi n}^{(1)}$ for fixed cut-offs $\Lambda_{\rm reg}$ excluding three-body interactions. The horizontal shaded band represents our benchmark range of values of B_3 considered between the limits, $B_3 = 2.886$ MeV and 4.06 MeV, predicted by the Faddeev calculation based potential model analyses [39,43]. The vertical dotted line represents our choice of the input scattering length $a_{\Xi n}^{(1)} = 4.911$ fm, as predicted by the recently updated ESC08c Nijmegen potential model analyses [60,61]

of Ref. [43] and $B_3 = 4.06$ MeV of Ref. [39] at the cut-off scales $\Lambda_{\rm reg} \approx 334$ MeV and $\Lambda_{\rm reg} \approx 465$ MeV respectively. The same result is demonstrated more conspicuously in Fig. 5 where we plot the variation of the eigenenergy B_3 by (hypothetically) varying the scattering length $a_{\Xi n}^{(1)} > 0$ for several fixed cut-offs $\Lambda_{\rm reg}$ excluding 3BF terms. The chosen potential model predicted range, 2.886 MeV $\lesssim B_3 \lesssim 4.06$ MeV, as demarcated by the horizontal band in the figure, is well constrained within our regulator range, 334 MeV $\lesssim \Lambda_{\rm reg} \lesssim 465$ MeV. In particular, our summary Table 3 displays the $\Lambda_{\rm reg}$ values at which our EFT solutions reproduce several more of the existing Faddeev calculation based model predictions for the $\Xi^- nn$ binding energy [39,41–43]. Although the above regulator range apparently seems well beyond the expected $\text{\textpi}$EFT hard scale $\Lambda_H \sim m_\pi$, the model results may still be accommodated within the framework of a modified EFT having an extended domain of validity. Consequently, such a modified halo $\text{\textpi}$EFT should have a larger breakdown scale, say, $\widetilde{\Lambda}_H \lesssim 500$ MeV, where interactions between the Ξ-hyperon and neutron are possibly dominated by two-pion ($\pi\pi$) or σ-meson exchange mechanisms. We note that one-pion-exchanges are typically ruled out by isospin invariance in strong processes.

Finally, we give a simple demonstration of predictability of our EFT framework. To this end, we attempt a *naive* estimation of the $\Xi^- nn$ ($I = 3/2$, $J = 1/2$) three-body scattering length, or more precisely the $n - (\Xi^- n)_t$ elastic S-wave scattering length a_3, by utilizing the potential model predicted three-body binding energy information from Refs. [39,41–43]. Here we need

to solve our coupled STM integral Eqs. (13) and (14) in the kinematical scattering domain. Subsequently, the three-body scattering length is obtained by considering the on-shell threshold limit of the renormalized elastic scattering amplitude $t_A^{(R)}$ [cf. Eq. (18)]. Solving the STM equations with the 3BF terms excluded (i.e., with $g_3 = 0$) leads to strong regulator dependence with the resulting amplitude displaying quasi-periodic singularities akin to the limit cycle behavior (cf. left panel of Fig. 6). Such divergences are renormalized by introducing the 3BF counterterms with the running coupling $g_3(\Lambda_{\rm reg})$ already fixed using the RG limit cycles corresponding to model predicted B_3 inputs (cf. Fig. 3).

Figure 6 (right panel) depicts the regulator dependence of the three-body scattering length $a_3(\Lambda_{\rm reg})$ renormalized by the 3BF terms. As mentioned, the scale dependence of the 3BF coupling $g_3(\Lambda_{\rm reg})$ is fixed using the RG limit cycles corresponding to the potential model inputs for B_3 [39,43]. The renormalized plots still exhibit a residual regulator dependence stemming from the low cut-off scale sensitivity of the counterterms owing to the decoupling of most underlying physics. However, for sufficiently large cut-off, say $\Lambda_{\rm reg} \gtrsim 400$ MeV, most of the underlying low-energy three-body dynamics are well captured in our solutions to the integral equations. Consequently, renormalizing a_3 using the counterterms becomes more effective at large $\Lambda_{\rm reg}$ leading to a well-defined asymptotic limit:

$$a_3^\infty = \lim_{\Lambda_{\rm reg} \to \infty} a_3(\Lambda_{\rm reg}). \qquad (22)$$

Hence, for each B_3 input a constant value a_3^∞ is obtained, as demanded by renormalization invariance, representing our predicted three-body scattering length. In particular, our limiting benchmark inputs, $B_3 = 2.886$ MeV and 4.06 MeV, lead to $a_3^\infty = 4.860$ fm and 2.573 fm respectively. In addition, our summary Table 3 displays some intermediate results corresponding to two other existing model predictions, namely, $B_3 = 3.89$ MeV and 3.00 MeV, from the Faddeev calculations analyses of Refs. [41,42]. Here we point out that for possible negative choice of the $^3S_1$ $\Xi^- n$ scattering length, such as the two recent SU(3) chiral EFT predictions, namely, $a_{\Xi n}^{(1)} = -0.09, -1.17$ fm [56,57], the $(\Xi^- n)_t$ sub-system is unbound with no kinematical particle-dimer scattering domain below the three-particle break-up threshold, i.e., $E < 0$.

Our predicted range of three-body scattering lengths represents a *naive* ballpark estimate based on the induced universal correlations which are expected to manifest in a halo-bound $\Xi^- nn$ system, albeit approximations considered in the analysis. To elucidate one of the inherent universal features, it is worth demonstrating the B_3 versus a_3^∞ correlations corresponding to our preferred choice of the input $\Xi^- n$ scattering length, namely, $a_{\Xi n}^{(1)} = 4.911$ fm [60,61]. This yields the well-known Phillips line correlation plot for the $\Xi^- nn$ system, as depicted in Fig. 7. The curve diverges as $B_3 \to \mathcal{B}_2 = 1.47$ MeV, the $n + (\Xi^- n)_t$ particle-triplet-dimer threshold, whenever an Efimov-like bound state

590

Eur. Phys. J. Spec. Top. (2021) 230:579–601

Table 3 Summary of our EFT results with three different input S-wave $^3S_1$ Ξ^-n scattering lengths, namely, $a^{(1)}_{\Xi n} = 4.911$ fm, taken from the updated ESC08c Nijmegen model analyses [60,61], $a^{(1)}_{\Xi n} = -0.09$ fm, taken from the relativistic LO chiral EFT analysis [56], and $a^{(1)}_{\Xi n} = -1.17$ fm, taken from the NLO chiral EFT-based non-relativistic G-matrix analysis [57]

Scattering length $a^{(1)}_{\Xi n}$ (fm)	Binding energy B_3 (MeV)	Cut-off $\Lambda^{(g_3=0)}_{\mathrm{reg}}$ (MeV)	Scattering length a_3^∞ (fm)
4.911 (Nijmegen model) [60,61]	2.886 [43]	334	4.860
	2.89 [41]	335	4.849
	3.00 [42]	348	4.562
	4.06 [39]	465	2.573
−0.09 (Relativistic Chiral EFT) [56]	2.886 [43]	22590	–
	2.89 [41]	22591	–
	3.00 [42]	22595	–
	4.06 [39]	22633	–
−1.17 (G-matrix Chiral EFT) [57]	2.886 [43]	2333	–
	2.89 [41]	2334	–
	3.00 [42]	2345	–
	4.06 [39]	2440	–

Displayed are the regulator scales $\Lambda^{(g_3=0)}_{\mathrm{reg}}$ at which the Efimov ground state eigenenergy (by excluding g_3) reproduces each of several existing potential model predictions on the three-body binding energies B_3 of the Ξ^-nn system [39,41–43]. Also summarized are our predicted three-body scattering length (a_3^∞) values corresponding to each model input for B_3, with the three-body coupling $g_3(\Lambda_{\mathrm{reg}})$ determined by the respective RG limit cycles. The results corresponding to the $a^{(1)}_{\Xi n} < 0$ scenario have no kinematical particle-dimer scattering domain for $E < 0$ and the three-body system is likely to remain unbound. In contrast, the $a^{(1)}_{\Xi n} > 0$ scenario shows encouraging prospect for a physically realizable Ξ^-nn Efimov state
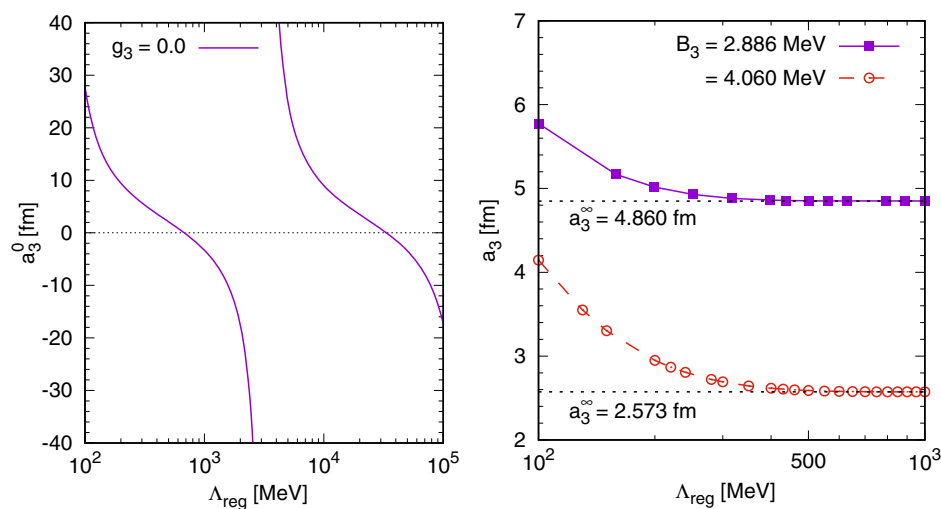

Fig. 6 Regulator (Λ_{reg}) dependence of the $n - (\Xi^-n)_t$ elastic S-wave three-body scattering length a_3, obtained by solving the coupled integral Eqs. (13) and (14) with input S-wave scattering length $a_{\Xi n} = 4.911$ fm, taken from the updated Nijmegen model analyses [60,61]. Left panel: The unrenormalized scattering length $a_3 \to a_3^0$ excluding the three-body coupling, i.e., $g_3 = 0$. Right panel: The renor-malized scattering length including the three-body coupling $g_3 \neq 0$. The scale dependence of $g_3(\Lambda_{\mathrm{reg}})$ is determined using the respective RG limit cycles (cf. Fig. 3) corresponding to the two three-body inputs, $B_3 = 2.886$ MeV and 4.06 MeV, taken from the Faddeev calculation model analyses [39,43]. Our predictions, namely, $a_3^\infty = 4.860$ fm and 2.573 fm, correspond to the respective asymptotic limits

emerges at zero-energy threshold (i.e., with $B_d = B_3 - \mathcal{B}_2 = 0$). A second virtual bound three-body state with large negative value of a_3^∞ is expected to emerge around $B_3^{(\mathrm{virt})} = e^{\pi/s_0}\mathcal{B}_2 \approx 70$ MeV, where the Phillips line diverges again. However, the latter state lies outside the

domain of validity of standard $^\#$EFT with an estimated breakdown energy scale $-E_{\mathrm{break}} \sim 14$ MeV, as determined by the three-body binding momentum of the order of the pion mass, i.e., $\gamma_3 = \sqrt{-2\mu_{n(n\Xi)}E_{\mathrm{break}}} \sim m_\pi$. The four data points displayed in the figure correspond to the B_3 predictions from the potential model
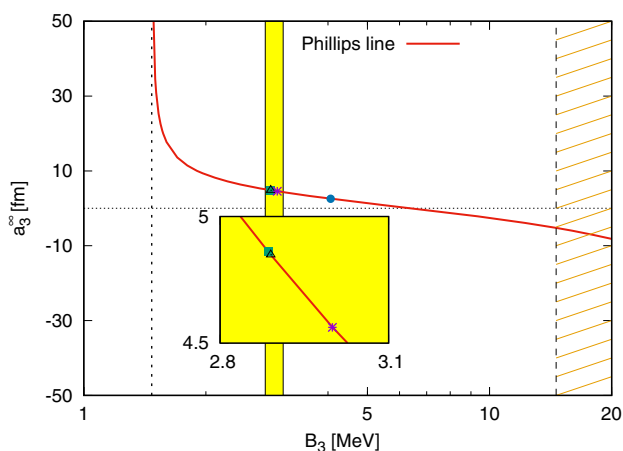
Eur. Phys. J. Spec. Top. (2021) 230:579–601

591

Fig. 7 Phillips line correlation for the $(I = 3/2, J = 1/2)$ $\Xi^- nn$ system corresponding to the input $^3S_1$ $\Xi^- n$ scattering length $a_{\Xi n}^{(1)} = 4.911$ fm, as predicted by the updated ESC08c Nijmegen model analyses [60,61]. The data points correspond to the input values of the three-body binding energy $B_3 = 2.886$ MeV, 2.89 MeV, 3.00 MeV and 4.06 MeV, predicted by the potential model analyses [39,41–43]. The vertical dotted line on the left represents the $n + (\Xi^- n)_t$ particle-dimer threshold at $B_3 = \mathcal{B}_2 = 1.47$ MeV, while the hashed region, $B_3 \gtrsim 14$ MeV, represents the expected breakdown region of our halo EFT description

analyses [39,41–43], all of which rely on the same two-body input from the Nijmegen model analyses, namely, $a_{\Xi n}^{(1)} = 4.911$ fm [60,61] (cf. Table 3). The fact that the Phillips plot evidently reflects certain degree of compatibility of the potential model inputs with our EFT description is an important qualitative finding of this work. In the event of possible future availability of phenomenological three-body data, a more rigorous NLO EFT analysis (explicitly including effective range terms) may be helpful to substantiate such connections on a better footing.

5 Summary and conclusions

A knowledge of few-body dynamics in light $(S = -2)$ Ξ-hypernuclei can serve as an essential input to the neutron star EoS for possible explanation of their stabilities with masses $\gtrsim 2M_\odot$. In this regard, the $\Xi^- nn$ $(I = 3/2, J^P = 1/2^+)$ three-body system is one of the simplest systems to investigate the nature of the underlying 3BF. The reason being the stability of this channel against strong decays and the absence of Coulomb interactions. However, the impracticability of performing Ξ-hyperon scattering experiments and the lack of empirical data thereof have so far eluded rigorous determination of essential few-body observables. Thus, a general qualitative insight relying solely on low-energy universality is needed to illuminate specific characteristics of the underlying interactions that may reflect the emergence of exotic halo-bound states.

Here we used the framework of leading order halo $\#$EFT in a speculative study to explore the feasibility that the $\Xi^- nn$ system is Efimov-bound. Notably, the presence of the predominantly repulsive $^1S_0$ $\Xi^- n$ sub-system channel potentially leads to the generation of anomalously deep two- and three-body unphysical bound states beyond the breakdown scale of the theory. In our current simplistic approach, as a first approximation, such unphysical contributions are avoided on an *ad hoc* basis by explicitly decoupling this channel in the construction of our integral equations. Our asymptotic analysis of the $\Xi^- nn$ integral equations revealed the formal appearance of Efimov states in the unitary limit associated with an RG limit cycle with a discrete scaling factor, $s_0^\infty = 0.803391\ldots$. The factor, however, differs from the expected value $(s_0^\infty)_{\text{expect}} \approx 1.01$, as governed by the universality of three-particle mass ratios [68], owing to the decoupling of the $^1S_0$ $\Xi^- n$ channel. Such scaling differences can certainly influence various numerical estimates in the low-energy non-asymptotic domain, but the general qualitative features are likely to remain unchanged with the inclusion of both the spin channels.[9]

Evidently, the unavailability of empirical three-body datum to fix the scale dependence of the three-body coupling $g_3(\Lambda_{\text{reg}})$ is a major drawback of our approach which prevents robust predictions. Thus, we relied on several existing Faddeev calculation based potential model analyses [39,41–43] for the input three-body binding energy B_3 in the reasonable benchmark range, $2.886-4.06$ MeV. Moreover, the $\#$EFT formalism requires the two-body inputs, namely, the $^1S_0$ nn scattering length $a_{nn} = -18.63$ [112], and the $^3S_1$ $\Xi^- n$ scattering length $a_{\Xi n}^{(1)}$. For the choice of the latter, we considered two contrasting scenarios, given the current ambiguities in regard to the underlying nature of the interactions in spin–isospin triplet $(1,1)$ $\Xi^- n$ channel. In the first scenario we considered the prediction, $a_{\Xi n}^{(1)} = 4.911$ fm, from the recently updated Nijmegen model analyses [60,61], which is based on the notion of a strongly attractive likely bound $(\Xi^- n)_t$ sub-system. In the second scenario we considered the predictions of two contemporary SU(3) chiral EFT analyses, namely, $a_{\Xi n}^{(1)} = -0.09$ fm [56], based on a relativistic calculation, and $a_{\Xi n}^{(1)} = -1.17$ fm [57], based on a non-relativistic in-medium G-matrix calculation, both concurring on a moderately attractive nature of the $(\Xi^- n)_t$ sub-system channel. With both the chiral EFT inputs, our investigations hinted at a predominantly unbound $\Xi^- nn$ system. In contrast with the input, $a_{\Xi n}^{(1)} = 4.911$ fm, the first scenario indicated favourable prospects for a physically realizable $\Xi^- nn$ Efimov-like ground, with the proviso that our $\#$EFT formalism could be extended (with $\tilde{\Lambda}_H \gtrsim 500$ MeV) to accommodate interactions

---

[9] In either cases we expect to find robust three-body universal features, such as the quasi-periodic RG limit cycle behavior of the three-body coupling and the induced Phillips line correlations.

mediated by $\pi\pi$ or σ-meson exchanges. Specifically, our eigensolutions (B_3) to the integral equations (excluding the 3BF terms) could reproduce the benchmark range of model inputs for the cut-off regulator values in the range $\Lambda_{\rm reg} \approx 335-464$ MeV.

Finally, as a simple demonstration of the predictive power of our EFT formalism we evaluated the three-body S-wave $n - (\Xi^- n)_t$ scattering length to lie in the range, $a_3^\infty \approx 2.6-4.9$ fm, corresponding to the same aforementioned benchmark range of model inputs for B_3. Given the very speculatory nature of the present study and the indeterminable three-body scattering length from present day experiments, the numerical figures for a_3^∞ are by all means *naive* ballpark estimates. Nevertheless, they are indicative of the emergent universal features of a prospective Efimov-bound $\Xi^- nn$ system which induce three-body correlations like the Phillips line. Such universal three-body features are robust against ambiguities in the two-body description given that the three-body datum is reliable. Consequently, our obtained results reasonably guesstimate similar qualitative results expected from more rigorous $\not\pi$EFT-based future investigations with systematic inclusion of both $\Xi^- n$ sub-system spin channels. Needless to emphasize that our conclusions tacitly relied on the presumed halo-bound structure of the $\Xi^- nn$ system, *viz.* a strongly attractive and bound $^3S_1$ $\Xi^- n$ sub-system and a predominantly weak (attractive or repulsive) $^1S_0$ $\Xi^- n$ sub-system with small scattering length.

A more systematic (realistic) approach requires a modification of the dibaryon formalism of the $\not\pi$EFT power counting, as well as including subleading order range effects. However, such a modified EFT analysis is beyond the scope of the present work and must be certainly explored as a possible future endeavor when more data will become available from upcoming experiments, such as ALICE [47] and FAIR [48]. Moreover, a next-to-leading order analysis would involve additional unknown three-body parameters in the theory thereby requiring more empirical inputs which are currently unprocurable.

A Efimov physics in low-energy EFT

For the sake of pedagogical completeness, we highlight aspects of the halo EFT analysis of two- and three-body universality responsible for formation of exotic Efimov-like states in *fine-tuned* three-body systems. *Universality* in this context refers to the property of *distinct separation of scales*, namely, similarities in long-range (low-energy) characteristics of a large class of multi-particle systems which are insensitive to the short-distance (high-energy) details. The halo-bound systems typi-

cally satisfying this property are naturally suited for a low-energy EFT description. We elucidate the pertinent EFT framework using the simplest system of three *identical* interacting spinless bosons ($B-B-B$), where additional involvement of spin and isospin degrees of freedom are absent. In particular, we consider a zero-range "toy-model" (ZRM) scenario (i.e., with two-body interaction range $r_0 \to 0$) which motivates the general formalism of a leading order EFT analysis implemented in this paper. The foundations to this framework have been extensively discussed in the context of a large collection of pionless EFT ($\not\pi$EFT) works in the literature (see, e.g., [2,68,72–83] and references therein). For the ensuing discussions below, we closely follow the reviews works [68,83,117].

A.1 Two-body sector

The two-body dynamics stems from the most general non-relativistic effective Lagrangian constituting all possible local short-range S-wave two-body interactions of the generic form [75–79]

$$\mathscr{L}_2^{\rm (KSW)} = B^\dagger \left[i\partial_t + \frac{\nabla^2}{2m_B} \right] B - \frac{C_0}{4} \left(B^\dagger B \right)^2 - \frac{C_2}{4} \left[\nabla (B^\dagger B) \right]^2 + \cdots, \qquad (23)$$

where the ellipses denote higher order derivative terms and $C_{0,2,\ldots}$ are two-body coupling constants. These couplings may be fixed from the empirical knowledge of the two-body parameters, such as those occurring in the well-known Bethe's *Effective Range Expansion* (ERE) formula for the S-wave scattering phase-shift δ_0, namely,

$$k \cot \delta_0 = -\frac{1}{a_0} + \frac{r_0}{2} k^2 + \mathcal{O}(k^4), \qquad (24)$$

with k being the center-of-mass scattering momentum of the two-boson ($B - B$) system. Especially, in the vicinity of shallow two-body (real or virtual) bound states these couplings are subject to an *unnatural scaling* with the magnitude of the S-wave scattering length (a_0) becoming unusually large in comparison to the short-distance effective range (r_0) of the interactions. In this case the theory becomes approximately conformally invariant, leading to a peculiar EFT governed by a non-trivial RG fixed point of the scale-dependent couplings [82].

Consider Q to be a generic small momentum associated with a certain emergent low-energy scale γ_0 of the two-body system, and M_{hi} as the UV cut-off or the breakdown scale of the theory associated with the unresolved "heavy" pion mass m_π. Then, the unnatural scaling scenario implies $k \sim Q \sim \gamma_0 \sim 1/|a_0| \ll M_{hi} \sim 1/r_0$. This is distinguished from the natural scenario where the interaction range $r_0 \sim 1/m_\pi$ solely accounts for all relevant scales such that $k \sim Q \sim \gamma_0 \sim 1/|a_0| \sim M_{hi} \sim 1/r_0$. Such unnatural two-body systems
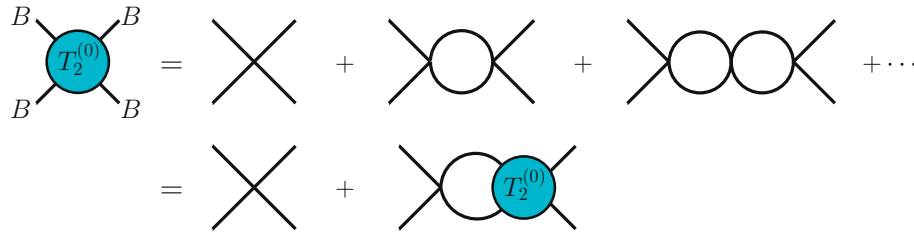
Fig. 8 The leading order two-body S-wave scattering amplitude $T_2^{(0)}$, obtained by resumming of the "bubble" graphs containing the C_0 interaction. It is compactly represented as a Lippmann–Schwinger integral equation, $\hat{T}_2^{(0)} = \hat{V}_2 + \hat{V}_2 \hat{G}_0 \hat{T}_2^{(0)}$

are ubiquitous in nuclear physics, say, in the case of two neutrons, $a_{nn} = -18.63$ fm $\gg r_{nn} \sim 1/m_\pi \sim 0.5$ fm. In all these manifestly *fine-tuned* scenarios near-threshold (shallow) bound *dimer* states emerge by critically tuning the couplings according to

$$C_{2r} \sim \frac{1}{2\mu_B M_{hi}^r Q^{r+1}} \quad \forall r \in \mathbb{Z}_+ \qquad (25)$$

with $\mu_B = m_B/2$ being the reduced mass of the two-boson $(B - B)$ system. This kind of two-body contact interactions scaling rule is termed as the *Q-counting* [76–80]. Based on the Q-counting different components of Feynman amplitudes scale as follows:

– the non-relativistic boson propagator, namely,

$$iS_B(p) = \frac{i}{p_0 - \frac{\mathbf{p}^2}{2m_B} + i\eta}, \qquad (26)$$

scales as $\sim m_B/Q^2 \sim \mathcal{O}(Q^{-2})$,
– the loop integral scales as $\sim \mathcal{O}(Q^5)$, [10]
– the interaction vertices $C_{2r}\nabla^{2r}$ scale as $\sim \mathcal{O}(Q^{r-1})$.

Accordingly, all two-body Feynman graphs contributing up to a fixed order in the counting, say $\mathcal{O}(Q^N)$, with L loops and $\mathcal{V}_{2r}$ interaction vertices with $2r$ derivatives scale as [117]

$$T_2^{(N)} = \sum_{\nu=-1}^{N} T_2^{(\nu)}, \quad T_2^{(\nu)} \sim \mathcal{O}(Q^\nu) \,;$$
$$\nu = 3L + 2 + \sum_{r=0} (r-3)\mathcal{V}_{2r} \geq -1 \,. \qquad (27)$$

Thus, for example, at low energies $E \sim 1/a_0^2$, restricting to leading order in Q-counting (i.e., for $N = -1$), an infinite number of loops with only C_0 interactions are needed to be non-perturbatively resummed. Such an infinite sequence of "bubble diagrams", all contributing

at the same order in the Q-counting (cf. Fig. 8), yields a shallow two-body bound state. However, at the next order (i.e., for $N = 0$) the C_2 interactions contribute to the dynamics. Being $1/M_{hi}$ suppressed compared to the leading C_0 interactions, the C_2 constitutes a perturbative correction. Such a "bubble resummation" with only the C_0 interaction leads to a *Lippmann–Schwinger series* for the two-body scattering amplitude $T_2^{(0)}$ which may be expressed as an integral equation:

$$T_2^{(0)}(E) = -C_0 - \frac{1}{2}C_0 \int \frac{d^4q}{(2\pi)^4 i} \frac{i}{q_0 - \mathbf{q}^2/2m_B + i\eta}$$
$$\times \frac{i}{E - q_0 - \mathbf{q}^2/2m_B + i\eta} T_2^{(0)}(E) \,, \qquad (28)$$

where q_0, $\mathbf{q}$ are temporal and spatial parts of loop four-momentum q. The integral equation may be regularized using a sharp momentum cut-off Λ_{reg} and subsequently solving to obtain

$$T_2^{(0)}(E, \Lambda_{\text{reg}}) = -C_0 \left[1 + \frac{\mu_B C_0}{2\pi^2} \left(\Lambda_{\text{reg}} - \frac{\pi}{2}\sqrt{-2\mu_B E - i\eta} \right) \right]^{-1}. \qquad (29)$$

The renormalization of the amplitude $T_2^{(0)}(E)$ can be implemented by matching to the two-body S-wave scattering length using the relation

$$a_0 = -\frac{\mu_B}{4\pi} \lim_{k \to 0} T_2^{(0)}(E = \mathbf{k}^2/2\mu_B) \,, \qquad (30)$$

leading to the regulator-dependent result for the coupling C_0, namely,

$$C_0(\Lambda_{\text{reg}}) = \frac{4\pi a_0}{\mu_B} \left(1 - \frac{2a_0 \Lambda_{\text{reg}}}{\pi} \right)^{-1}, \qquad (31)$$

such that the renormalized scattering amplitude is given by

$$T_2(E) = \frac{4\pi}{\mu_B} \frac{1}{-1/a_0 + \sqrt{-2\mu_B E - i\eta}} \,. \qquad (32)$$

Auxiliary field formalism In the context of studying three-body dynamics with two-body bound subsystems

---

[10] This is easily seen as follows:

$$\int d^4q \sim \int dq_0 \int d^3\mathbf{q} \sim \frac{Q^2}{2\mu_B} \cdot Q^3 = \frac{Q^5}{2\mu_B} \,.$$

594

Eur. Phys. J. Spec. Top. (2021) 230:579–601

with large scattering lengths, it is convenient to introduce auxiliary *dimer* fields or *dimerons* (d). Ideally, the bare auxiliary fields do not propagate and even have a "wrong sign" in the kinetic terms (see following two-body Lagrangian). Hence, the content of the original theory remains unchanged by the addition of such ghost fields "by hand". For the present case of the spinless three-boson system ($B - B - B$), an alternative two-body Lagrangian in terms of the dimeron fields can be constructed as [72–74],

$$\mathscr{L}_2^{(\text{BHvK})} = B^\dagger \left[i\partial_t + \frac{\nabla^2}{2m_B} \right] B - d^\dagger \left[i\partial_t + \frac{\nabla^2}{4m_B} - \Delta_d \right] d$$
$$- y_0 \left(d^\dagger B^2 + B^{\dagger 2} d \right) + \cdots . \quad (33)$$

In effect, the dimerons are essentially employed to cancel the quadratic terms such as $(B^\dagger B)^2$ in Eq. (23), so that all interactions between the B fields are now mediated *via* the dimer exchange process, with y_0 as the corresponding interaction coupling. The quantity Δ_d is a free parameter related to the binding energy of the dimeron d such that the bare or tree-level dimeron propagator is the simple non-dynamical term i/Δ_d. Quantum loop corrections, however, allow the dimerons to propagator. It is notable that by virtue of reparametrization invariance of the theory, the above Lagrangian can be shown to be equivalent to the original two-body Lagrangian, Eq. (23).

In the context of halo EFT where the dimeron formalism has been extensively used, the Q-counting scheme has been extended to include the scaling,

$$y_0^2 \sim \frac{M_{hi}}{4\mu_B^2} \sim \mathcal{O}(1) \quad \text{and} \quad \Delta_d \sim \frac{M_{hi}Q}{2\mu_B} \sim \mathcal{O}(Q). \quad (34)$$

Consequently, using field re-definitions in trading away the time derivatives in favor of space derivatives, the kinetic term becomes sub-leading compared to term proportional to Δ_d. In that case the Q-counting leads to an infinite sequence of Feynman graphs (similar to the ones displayed in Fig. 1), each contributing at the same order as the static dimeron propagator $i\Delta_d^{-1} \sim \mathcal{O}(Q^{-1})$. Consequently, they must all be resummed at the leading order to yield the full dynamical "dressed" dimeron propagator:

$$i\Delta^{(0)}(p_0, \mathbf{p}) = \frac{i\pi}{y_0^2 \mu_B} \left[\frac{\pi \Delta_d}{y_0^2 \mu_B} + \frac{2}{\pi} \Lambda_{\text{reg}} \right.$$
$$\left. - \sqrt{-2\mu_B p_0 + \mathbf{p}^2/4 - i\eta} \right]^{-1} . \quad (35)$$

We note its similarity to the resummed two-body scattering amplitude, Eq. (29), with the two-body center-of-mass kinetic energy $E \to p_0 - \mathbf{p}^2/(8\mu_B)$, where $p_0(\mathbf{p})$ is kinetic energy (momentum) of the dimeron. Upon renormalization using Eq. (31) and the leading order relation among the two-body parameters, namely,

$C_0 \to 4y_0^2/\Delta_d$, the renormalized dressed dimeron propagator becomes

$$i\Delta(p_0, \mathbf{p}) = -\frac{i\pi}{y_0^2 \mu_B} \left[-\frac{1}{a_0} + \sqrt{-2\mu_B p_0 + \mathbf{p}^2/4 - i\eta} \right]^{-1} . \quad (36)$$

If scattering length $a_0 > 0$, then the above dimeron propagator has a pole at $p_0 = -1/(2\mu_B a_0^2) + \mathbf{p}^2/(8\mu_B)$. For low-energy threshold processes, $\mathbf{p} \to 0$ and $p_0 \to -\mathcal{B}_2 = -1/(2\mu_B a_0^2)$, in which case the renormalized dimeron propagator has a residue (wave function renormalization constant) at the pole given by

$$\mathcal{Z}_d = \left[\frac{\mathrm{d}\Delta_d^{-1}(p_0, \mathbf{0})}{\mathrm{d}p_0} \right]_{p_0 = -\mathcal{B}_2}^{-1} = \frac{2\pi}{y_0^2 \mu_B^2 a_0} . \quad (37)$$

A.2 Three-body sector

Here we describe the dynamics associated with S-wave scattering of the three-boson system depicted in Fig. 9. Excluding the *genuine* three-body interaction (3BF) diagrams shown in the second row, the scattering diagrams in the first row constitute only the two-body interaction y_0, and thus described by same leading order EFT Lagrangian, Eq. (33). Under the Q-counting scheme, a simple investigation shows that these diagrams contribute at the same order. For example, the tree level diagram in first row can be considered as a one-boson (B) exchange process between the incoming and outgoing dimerons (d). Since the tree diagram containing two dBB vertices ($y_0^2 \sim M_{hi}/4\mu_B^2$) and one B propagator ($iS_B \sim m_B/Q^2$), this amounts to a net contribution of order $\sim M_{hi}/(2\mu_B Q^2)$. The adjacent one-loop re-scattering diagram contains two additional dBB vertices, two additional B propagators, a dimeron propagator ($i\Delta \sim 2\mu_B/M_{hi}Q$), and a loop integral ($\sim Q^5/2\mu_B$). This implies that the one-loop diagram also scales as $\sim M_{hi}/(2\mu_B Q^2)$, like the tree graph. In fact, inspection shows that every re-scattering graph in the first row precisely contributes at the same leading order, necessitating a resummation of all such graphs. Besides, one also requires the infinite sequence of 3BF diagrams (second row) which may be shown to contribute at the leading order, and hence needed to be resummed as well. The power counting for such graphs is described later in this section. However, unlike the resummation in the two-body sector [cf. Eq. (28)] which amounts to a simple summation of a geometric series, the same is impracticable in the three-body sector. In contrast, here we must incorporate a non-perturbative resummation in the form of a "one-loop" Fredholm integral equation (third row of Fig. 9) which is solved self-consistently for the scattering amplitude $T_3^{(0)}$ using numerical methods. It is notable that
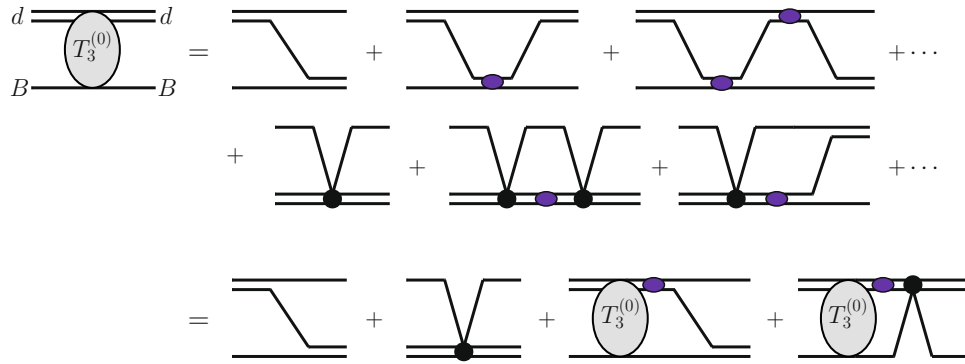
Fig. 9 Diagrammatic representation of the three-body integral equation for the spinless three-boson S-wave scattering amplitude $T_3^{(0)}$. In the Q-counting scheme, all graphs in the first line contribute as $\sim M_{hi}/(2\mu_B Q^2)$, while those in the second line with three-body contact interactions contribute as $\sim 1/(2\mu_B Q^4)$. The single line denotes a boson (B) propagator, the double line denotes a static dimeron (d) propagator, and the double line with an oval blob represents a fully dressed (dynamical) renormalized dimeron propagator. Finally, the dark filled circle represents an insertion of a leading order three-body contact interaction

the standard Faddeev equations[11] are a set of coupled integro–differential equations in the co-ordinate representation. They are numerically solved using finite range model potentials with well-defined kernels in the Hilbert-Schmidt class. Our ZRM integral equations in contrast have an ill-defined kernel stemming from the non-self-adjoint character of the underlying three-body Hamiltonian [84,85,119,120]. Such "Faddeev-like" zero range three-body integral equations in the momentum representation are termed as the STM or the so-called Skornyakov–Ter–Martirosyan equations [69–71]. Despite the ambiguities in their solution, the STM

equations have the primary advantage of fitting naturally into an EFT framework based on a diagrammatic or Lagrangian-based approach. This contrasts with the inherently non-perturbative Hamiltonian-based potential model approach for solving three-body Faddeev equations.

The biggest advantage, however, lies in the manner of introducing 3BF which is quite naturally achieved in the STM framework without the requirement of *ad hoc* three-body potentials. The ambiguity in the Hamiltonian is solved by cutting off the effective interactions at short-distances. This is accomplished in the EFT by introducing, e.g., a sharp momentum cut-off Λ_{reg} in the integral equations which becomes a free parameter of the theory. This regularization method implicitly necessitates the introduction of cut-off-dependent three-body couplings needed to renormalize the artificial cut-off dependence of the STM equations. To this end, we introduce additional non-derivatively coupled three-body interactions in the effective Lagrangian, for instance,

$$\mathscr{L}_3^{(\mathrm{KSW})} = \frac{D_0(\Lambda_{\mathrm{reg}})}{36}(B^\dagger B)^3 + \cdots, \quad (\text{standard form})$$

$$\mathscr{L}_3^{(\mathrm{BHvK})} = -d_0(\Lambda_{\mathrm{reg}})\left(d^\dagger d\right)\left(B^\dagger B\right) + \cdots, \quad (\text{dimerized form})$$

$$(38)$$

with the contact interaction couplings scaling unnaturally at the leading order, namely, $D_0 \sim d_0 \sim 1/(2\mu_B Q^4)$. In this case the $B - B - B$ system exhibits three-body (Efimov) universality.[12] The values of the 3BF couplings can be fixed using additional three-body

---

[11] The Faddeev equations, as distinct from the three-particle Schrödinger equation, is a set of three coupled channel equations tailor-made to exploit configurations consisting of a two-body cluster that is well-separated from the third particle, leading to considerable simplifications in the solution. Moreover, at low-energies ignoring the subsystem angular momentum follows more naturally than in Schrödiger equation. With considerable simplifications they reduce to a single integro-differential equation for the three-boson wavefunction $\psi(R, \alpha)$, with *hyperradius R* and generic *Delves' hyperangle $\alpha \equiv \alpha_k$* , defined by $R = \frac{1}{2}r_{ij}^2 + \frac{2}{3}r_{k,ij}^2$ and $\alpha_k = \arctan\left(\sqrt{3}r_{ij}/2r_{k,ij}\right)$ respectively, in Jacobi coordinates, where (i, j, k) is a cyclic permutation of $(1, 2, 3)$. This leads to the so-called low-energy Faddeev equation [68,118]:

$$(T_R + T_\alpha - E)\psi(R, \alpha) = -V(\sqrt{2}R\sin\alpha)\Bigg[\psi(R, \alpha)$$
$$+ \frac{4}{\sqrt{3}}\int_{|\frac{\pi}{3}-\alpha|}^{\frac{\pi}{2}-|\frac{\pi}{6}-\alpha|} \frac{\sin(2\alpha')}{\sin(2\alpha)}\psi(R, \alpha')\mathrm{d}\alpha'\Bigg],$$

with $\quad T_R = -\frac{1}{4\mu_B}\left[\frac{\partial^2}{\partial R^2} + \frac{5}{R}\frac{\partial}{\partial R}\right],$

$T_\alpha = -\frac{1}{4\mu_B R^2}\left[\frac{\partial^2}{\partial \alpha^2} + 4\cot(2\alpha)\frac{\partial}{\partial \alpha}\right].$

[12] For "natural" systems without three-body universality, the scaling of the 3BF couplings are instead governed by *naive* dimensional analysis (NDA), $D_0 \sim d_0 \sim 1/(2\mu_B M_{hi}^4)$. Thus, the corresponding 3BF terms are considered subleading in the EFT Lagrangian.

datum (e.g., three-body binding energy) in realistic situations. The ellipses denote derivative 3BF terms which are naturally subleading. Figure 9 (second row) displays all re-scattering diagrams with insertions of leading order three-body contact interactions. These graphs are similarly resummed into an integral equation that yields contributions of order $\sim 1/(2\mu_B Q^4)$, and hence equally important as the set of graphs in the first row with two-body interactions only. Together they constitute all possible non-perturbative contributions to the scattering amplitude at leading order.

Assuming the manifestation of Efimov universality, the natural choice of the reference frame is the boson-dimeron $(B-d)$ center-of-mass (CM), with the relative external momenta being $-\mathbf{k}, \mathbf{k}$ $(-\mathbf{p}, \mathbf{p})$ for the incoming (outgoing) boson and dimeron respectively. With the total three-body CM kinetic energy as E, their energies are taken as E_A, $E - E_A$ $(E'_A, E - E'_A)$ for the incoming (outgoing) particles. Using standard Feynman rules which follow from the EFT Lagrangians, Eqs. (33) and (38), we easily obtain the following Faddeev-like STM integral equation for the unrenormalized scattering amplitude $T_3^{(0)}$ corresponding to the second line of Fig. 9, namely,

$$
\begin{aligned}
T_3^{(0)}(\mathbf{p}, \mathbf{k}; E) = &-\left[\frac{4y_0^2}{E - E'_A - E_A - (\mathbf{p}+\mathbf{k})^2/2m_B + i\eta}\right. \\
&\left. + d_0(\Lambda_{\text{reg}})\right] \\
&+ \frac{i\pi}{\mu_B y_0^2} \int^{\Lambda_{\text{reg}}} \frac{\mathrm{d}^4 q}{(2\pi)^4} \left[\frac{4y_0^2}{E - E'_A - q_0 - (\mathbf{p}+\mathbf{q})^2/2m_B + i\eta}\right. \\
&\left. + d_0(\Lambda_{\text{reg}})\right] \\
&\times \frac{1}{q_0 - \mathbf{q}^2/2m_B + i\eta} \frac{T_3^{(0)}(\mathbf{q}, \mathbf{k}; E)}{1/a_0 - \sqrt{-2\mu_B(E-q_0) + \mathbf{q}^2/4 - i\eta}},
\end{aligned}
$$

(39)

where $q_0(\mathbf{q})$ is the temporal (spatial) part of loop momentum with the three-momentum integral cut-off in the UV region at $|\mathbf{q}| = \Lambda_{\text{reg}}$. Using Cauchy's residue theorem, the integral over q_0 can be evaluated by choosing the pole, $q_0 = \mathbf{q}^2/2m_B$, making one of the boson propagators inside the loop integration on-shell. Further simplifications is achieved by choosing either one or both the initial and final states on-shell. For instance, with the full on-shell choice $E_A = \mathbf{k}^2/2m_B$ and $E'_A = \mathbf{p}^2/2m_B$, we obtain

$$
\begin{aligned}
T_3^{(0)}(\mathbf{p}, \mathbf{k}; E) = &-4m_B y_0^2 \left[\frac{1}{m_B E - (p^2 + \mathbf{p}\cdot\mathbf{k} + k^2) + i\eta}\right. \\
&\left. + \frac{d_0(\Lambda_{\text{reg}})}{4m_B y_0^2}\right] \\
&- 8\pi \int^{\Lambda_{\text{reg}}} \frac{\mathrm{d}^3 \mathbf{q}}{(2\pi)^3} \left[\frac{1}{m_B E - (p^2 + \mathbf{p}\cdot\mathbf{q} + q^2) + i\eta}\right. \\
&\left. + \frac{d_0(\Lambda_{\text{reg}})}{4m_B y_0^2}\right] \\
&\times \frac{T_3^{(0)}(\mathbf{q}, \mathbf{k}; E)}{-1/a_0 + \sqrt{-2\mu_B E + 3\mathbf{q}^2/4 - i\eta}}.
\end{aligned}
$$

(40)

Especially in the context of S-wave scattering process, we consider the projection of the unrenormalized amplitude onto the $l = 0$ partial wave renormalized amplitude given by

$$
T_3(p, k; E) \equiv \frac{\mathcal{Z}_d}{2} \int_{-1}^{1} \mathrm{d}\left(\cos\theta_{\hat{\mathbf{p}}\cdot\hat{\mathbf{q}}}\right) \; T_3^{(0)}(\mathbf{p}, \mathbf{k}; E) \, ,
$$

(41)

such that boson-dimeron *elastic* scattering amplitude is obtained by evaluating the renormalized scattering amplitude at the on-shell point, $p = |\mathbf{p}| = k = |\mathbf{k}|$ and $E = -\mathcal{B}_2 + 3k^2/(4m_B)$, with dimer binding energy $\mathcal{B}_2 = 1/(2\mu_B a_0^2)$. Furthermore, in the threshold limit one obtains the three-body scattering length as

$$
a_3^{(\text{Bd})} = -\frac{m_B}{3\pi} \lim_{k\to 0} T_3^{(0)}\left(k, k; \frac{3k^2}{4m_B} - \mathcal{B}_2\right). \quad (42)
$$

It is conventional to re-define the dimension-full three-body coupling $d_0(\Lambda_{\text{reg}})$ in terms of a dimensionless coupling $H(\Lambda_{\text{reg}})$ such that $T_3^{(0)}(p, k; E)$ has a well-defined asymptotic behavior as $\Lambda_{\text{reg}} \to \infty$, namely,

$$
d_0(\Lambda_{\text{reg}}) = -\frac{4m_B y_0^2}{\Lambda_{\text{reg}}^2} H(\Lambda_{\text{reg}}) \, . \quad (43)
$$

This leads to the 3BF renormalized STM integral equation for the three-boson system, originally derived in Ref. [74]:

$$
\begin{aligned}
T_3(p, k; E) = &\frac{8\pi}{\mu_B a_0} \left[\frac{1}{2pk} \ln\left(\frac{p^2 + k^2 + pk - m_B E - i\eta}{p^2 + k^2 - pk - m_B E - i\eta}\right)\right. \\
&\left. + \frac{H(\Lambda_{\text{reg}})}{\Lambda^2}\right] \\
&+ \frac{4}{\pi} \int_0^{\Lambda_{\text{reg}}} dq \; q^2 \left[\frac{1}{2pq} \ln\left(\frac{p^2 + q^2 + pq - m_B E - i\eta}{p^2 + q^2 - pq - m_B E - i\eta}\right)\right. \\
&\left. + \frac{H(\Lambda_{\text{reg}})}{\Lambda^2}\right] \\
&\times \frac{T_3(q, k; E)}{-1/a_0 + \sqrt{3q^2/4 - \mu_B E - i\eta}}.
\end{aligned}
$$

(44)

The above equation must be numerically solved to obtain the three-body eigenenergies and scattering lengths in the respective kinematical domains.[13] In this case the STM equation is one-dimensional in the sense that $B - d$ scattering involves a single channel elastic process $B + d \to B + d$. In realistic situations with non-zero spin–isospin degrees of freedom,

---

[13] It must be understood that the three-body bound states are obtained in the negative energy kinematical region, $E < \mathcal{E}_d$, namely below the boson-dimeron breakup threshold $\mathcal{E}_d \sim -\mathcal{B}_2$. While the $B - d$ scattering solutions correspond to energies, $\mathcal{E}_d \leq E < 0$, namely, the kinematical region in between the boson-dimeron and three-boson breakup thresholds.

the processes involve coupled elastic and inelastic channels, thereby requiring multi-dimensional representations. For instance, the $\Xi^- nn$ ($I = 3/2$, $J^P = 1/2^+$) system dealt in this paper involves a system of three coupled-channel scattering processes: the elastic channel $n + (\Xi^- n)_t \to n + (\Xi^- n)_t$, and the two inelastic channels $n + (\Xi^- n)_t \to n + (\Xi^- n)_s$ and $n + (\Xi^- n)_t \to \Xi^- + (nn)_s$, where the subscripts represent the subsystem spins. However, for the sake of simplicity the former inelastic channel involving the spin-singlet dimer $(\Xi^- n)_s$ is assumed to be decoupled (see text). Consequently, we deal with a reduced system of two coupled-channel integral equation in terms of the *half-on-shell* amplitudes $t_{A,B}^{(R)}$ (cf. Appendix B). Moreover, additional re-coupling coefficients are necessary for projecting each of the scattering diagrams onto the correct spin–isospin channels.

A.3 RG limit cycle

With sufficiently large $B - B$ scattering length, i.e., $a_0 \to \infty$, and very short range two-body interactions, $r_0 \to 0$, three-body or Efimov universality implies the existence of a tower of arbitrarily-shallow three-body bound states close to the unitary or resonant limit as $\Lambda_{\text{reg}} \to \infty$. This remarkable discovery is credited to Vitaly Efimov [86–88], who in 1970 demonstrated that the system of three identical bosons interacting *via* attractive (i.e, with $a_0 > 0$) inverse square channel potential $V \sim - \left(s_0^2 + 1/4 \right) / \mu_B R^2$ becomes resonant. By solving the Faddeev equations using the well-known *hyperspherical* representation in coordinate space with suitable short-distance *adiabatic* boundary conditions, a geometric sequence of three-particle level states (Efimov states) was obtained. The corresponding binding energies $B_3^{(n)}$ were found to lie approximately within the interval,

$$\frac{1}{2\mu_B a_0^2} \lesssim B_3^{(n)} \overset{n \to \infty}{\longrightarrow} \frac{\kappa_*^2}{2\mu_B} \left(e^{-2\pi/s_0} \right)^{(n-n_*)} \lesssim \frac{1}{2\mu_B r_0^2},$$
(45)

where $n = n_*$ is some integer labeling for a reference level with binding momentum κ_*, determined by the *Efimov spectrum* in the (asymptotic) unitary limit. The multiplicative factor $\lambda_0 \equiv e^{\pi/s_0}$ is an *universal parameter* which depends only on the gross features of the three-body system, such as the mass ratios of the bound particles and the overall quantum statistics of the system, irrespective of the fine details such as the nature of the individual bound particles and the short-distance interaction potentials. In this case, $s_0 = 1.00624\dots$ is obtained as a solution to the transcendental equation

$$s_0 \cosh \frac{\pi s_0}{2} = \frac{8}{\sqrt{3}} \sinh \frac{\pi s_0}{6}.$$
(46)

It is notable that mass ratios play the most crucial role in deciding the typical estimate for s_0. However,

the spin, isospin and other possible internal quantum numbers of the gross three-body system can fine-tune its precise value. Moreover, away from unitarity in the non-resonant domain as $a_0 \sim r_0$, the value of s_0 is likely to change from its asymptotic value due to cut-off and other low-energy parametric dependencies thereby becoming non-universal. For instance, the three-nucleon ($N - N - N$) iso-doublet S-wave systems of *triton* and *helion* (^{3}H, ^{3}He) in the $I = J = 1/2$ channel, are probably the best known examples of realistic Efimov-bound states in nuclear physics having identical asymptotic scale parameter s_0 and Efimov spectrum (neglecting Coulomb interactions) as in the case of the $B - B - B$ system.

The above-mentioned behavior of the three-body system in the so-called *scaling limit* ($r_0 \to 0$) is an indication that the familiar *continuous scaling* symmetry (conformal invariance) under the scale transformation

$$a_0 \to \lambda a_0 \qquad \text{and} \qquad E_{2-\text{body}} \to \lambda^{-2} E_{2-\text{body}},$$
(47)

where $\lambda \in \mathbb{R}_+$ is an arbitrary constant, gets evidently broken in the three-body sector into the *discrete scaling* subgroup of scale transformations given by

$$\kappa_* \to \kappa_* \quad a_0 \to \lambda_0^n a_0, \quad E \to \lambda_0^{-2n} E,$$
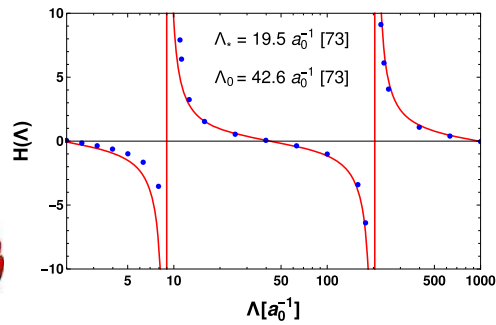$$\text{where } \lambda_0 = e^{\pi/s_0} \approx 22.7.$$
(48)

This feature can be attributed to the introduction of the parameter κ_* which sets a new relevant scale in the three-body system, in addition to the only existing relevant scale set by the two-body parameter $a_0 \to \infty$ close to the unitary limit. This leads to logarithmic scaling violation of low-energy observables which must scale as some log-periodic function $\sim f [s_0 \ln(\kappa_*|a_0|)]$. In other words, the expected non-trivial RG fixed point scaling of the 3BF couplings breaks down into that of an UV RG limit cycle discrete scaling characterized by the parameter λ_0. This unusual type of RG arises in other branches of physics as well, such as in condensed matter (see, e.g., Refs. [121–125]), or in the study of turbulence and complex systems (see e.g., Ref. [126]). Curiously enough, such a discrete scaling behavior bears close resemblance to the well-known Russian *Matryoshka* dolls, as displayed in Fig. 10. They consist of an assembly of hollow wooden dolls of decreasing size nested one within the other such that the ratio of the sizes of successive dolls remains approximately constant, for instance, as shown in the figure, the discrete scaling factor is given by

$$e^{2\pi/s_0^{(\text{doll})}} \approx \frac{\text{doll}^{(n)}}{\text{doll}^{(n+1)}} \approx 1.5.$$
(49)

Likewise, in proximity to the unitary limit, the ratio of the successive binding energies of the of $B - B - B$ Efimov *trimer* levels scale as $B_3^{(n)}/B_3^{(n+1)} \approx e^{2\pi/s_0} \approx 515$.

598

Eur. Phys. J. Spec. Top. (2021) 230:579–601

Fig. 10 Demonstration of RG limit cycle. Left panel: Discrete scaling behavior found in Russian nesting dolls with sizes of successive dolls decreasing by a constant factor ~ 1.5. Right panel: The regulator scale $\Lambda_{\rm reg}$ dependence of the three-body coupling $H(\Lambda_{\rm reg})$ for the $B-B-B$ sys-

tem. The input three-body datum is the scattering length $a_3^{(\rm Bd)} = 1.56a_0$. The parameters, Λ_* and Λ_0, are obtained by fitting Eq. (52) (solid curve) to the data points obtained by numerically solving the STM Eq. (44), reproducing the result of Ref. [74]

The approximate relation becomes an exact one only in the unitary limit with $a_0 = \infty$.

The RG limit cycle features associated with Efimov spectrum are deduced quite naturally in low-energy EFT by studying the cut-off regulator dependence of the 3BF coupling $H(\Lambda_{\rm reg})$ via the STM integral Eq. (44). The introduction of UV regulator $\Lambda_{\rm reg}$ repairs the non-self-adjoint pathology associated with the STM equation making the scattering amplitude T_3 well-behaved asymptotically. But this comes at a cost: the continuous scaling symmetry gets partially broken, leading to the emergence of an RG limit cycle. This feature can be checked analytically by investigating the asymptotic nature of the integral equation in the unitary and scaling limits. In other words, with p taken as the off-shell (outgoing) momentum having the same order of magnitude as the loop momenta q, we examine the integral equations in the limit $E, 1/|a_0|, k \ll p \sim q \sim \Lambda_{\rm reg} \lesssim \infty$, whereby the 3BF terms $\propto H(\Lambda_{\rm reg})/\Lambda_{\rm reg}^2$ may be dropped. To that effect, the asymptotic solution for T_3 scales as a pure power-law with an undetermined exponent, $T_3(p) \sim p^{s-1}$. Thus, the resulting STM Eq. (44) becomes

$$p^{s-1} = \frac{4}{\sqrt{3}\pi p} \int_0^\infty dq \; q^{s-1} \ln \frac{p^2 + pq + q^2}{p^2 - pq + q^2}, \quad (50)$$

which after a change of variable, $q = xp$, becomes

$$1 = \frac{4}{\sqrt{3}\pi} \int_0^\infty dx \; x^{s-1} \ln \frac{1 + x + x^2}{1 - x + x^2}. \quad (51)$$

A Mellin transformation finally reduces the STM equation to the very aforementioned transcendental relation, Eq. (46), obtained by solving the low-energy Faddeev equation, albeit with a complex exponent $s = \pm is_0$, where $s_0 = 1.00624\ldots$ is obtained in this case. The asymptotic value s_0 parametrizes the exact *discrete scaling* behavior at the unitary limit, formally indicating the manifestation of Efimov effect. Furthermore, Bedaque et al. [74] deduced an approximate analytical expression for the typical log-periodic running of

dimensionless three-body coupling $H(\Lambda_{\rm reg})$, given by

$$H(\Lambda_{\rm reg}) = -\frac{\sin\left[s_0 \ln(\Lambda_{\rm reg}/\Lambda_*) - \arctan(1/s_0)\right]}{\sin\left[s_0 \ln(\Lambda_{\rm reg}/\Lambda_*) + \arctan(1/s_0)\right]}. \quad (52)$$

Such an RG orbit for the coupling constant with a periodic dependence on the cut-off parameter when the latter increases to infinity is termed as a limit cycle. The underlying principle ensures that the family of effective theories with finite cut-offs yields predictions which are guaranteed to remain independent of the respective cut-offs. In the above expression Λ_*, in analogy to κ_*, is an emergent three-body dynamical parameter which results from the logarithmic scaling violation $\sim \ln(\Lambda_*|a_0|)$. This parameter is likewise fixed using a three-body datum, such as the trimer binding energy B_3 or the $B-d$ scattering length $a_3^{(\rm Bd)}$. Alternatively, the scale dependence of $H(\Lambda_{\rm reg})$ may be determined by numerically solving the STM Eq. (44) at non-asymptotic scales for a given two-body input a_0 and three-body datum (e.g., B_3, $a_3^{(Bd)}$, etc.). In Fig. 10, we reproduce the result of Ref. [74], displaying the approximate RG limit cycle with quasi-periodic singularities associated with the successive formation of new Efimov states as $\Lambda_{\rm reg} \to \infty$. The data points correspond to our numerical evaluations, while the solid curve is the fit to these data using the analytical formula of Bedaque et al., Eq. (52). To this end, one may extract the three-body parameters, such as Λ_* and s_0, using the momentum scaling relations,

$$\Lambda_n = \left(e^{\pi/s_0}\right)^n \Lambda_0 \quad \text{as } n \to \infty, $$

and

$$\Lambda_0 = \exp\left[\frac{\arctan(1/s_0)}{s_0}\right] \Lambda_*, \quad (53)$$

Eur. Phys. J. Spec. Top. (2021) 230:579–601

599

where $\Lambda_{\rm reg} = \Lambda_n$ represents the $n^{\rm th}$ zero of the three-body coupling $H(\Lambda_n)$. The typical non-asymptotic values of s_0 expected in this case depend on Λ_n, and hence differ from the cutoff-independent asymptotic value, $s_0 \to 1.00624\ldots$, which restores the exact scaling symmetry of the STM equation as $\Lambda_n \to \infty$.

B Integral equation for $\Xi^- nn$ $(I = 3/2, J^P = 1/2^+)$ system

The Faddeev-like three-body coupled integral equation for the $n + (\Xi^- n)_t \to n + (\Xi^- n)_t$ elastic scattering amplitude t_A (cf. Fig. 2) (excluding the $(\Xi^- n)_s$ singlet subsystem channel) can be easily obtained *via* Feynman rules from the non-relativistic effective Lagrangian, and is given as

$$
\begin{aligned}
t_A\left(\mathbf{p},\mathbf{k};E\right) = (-y_1^2) \Bigg[&\mathcal{C}_2^{(11)} S_\Xi \left(E - \frac{\mathbf{p}^2}{2M_n} - \frac{\mathbf{k}^2}{2M_n}, \mathbf{p}+\mathbf{k} \right) \\
&+ \mathcal{C}_3^{(11)} \frac{M_\Xi}{2} \frac{g_3(\Lambda_{\rm reg})}{\Lambda_{\rm reg}^2} \Bigg] \\
- \mathcal{C}_2^{(11)}(-y_1^2) &\int^{\Lambda_{\rm reg}} \frac{{\rm d}^3\mathbf{q}}{(2\pi)^3} t_A\left(\mathbf{q},\mathbf{k};E\right) S_\Xi \\
\times &\left(E - \frac{\mathbf{p}^2}{2M_n} - \frac{\mathbf{q}^2}{2M_n}, \mathbf{p}+\mathbf{q} \right) \\
\times &\mathscr{D}_1 \left(E - \frac{\mathbf{q}^2}{2M_n}, \mathbf{q} \right) \\
- \mathcal{C}_3^{(11)}(-y_1^2) \frac{M_\Xi}{2} &\int^{\Lambda_{\rm reg}} \frac{{\rm d}^3\mathbf{q}}{(2\pi)^3} t_A\left(\mathbf{q},\mathbf{k};E\right) \mathscr{D}_1 \\
\times &\left(E - \frac{\mathbf{q}^2}{2M_n}, \mathbf{q} \right) \frac{g_3(\Lambda_{\rm reg})}{\Lambda_{\rm reg}^2} \\
- \mathcal{C}_2^{(10)}(-y_0 y_1) &\int^{\Lambda_{\rm reg}} \frac{{\rm d}^3\mathbf{q}}{(2\pi)^3} t_B\left(\mathbf{q},\mathbf{k};E\right) S_n \\
\times &\left(E - \frac{\mathbf{p}^2}{2M_n} - \frac{\mathbf{q}^2}{2M_\Xi}, \mathbf{p}+\mathbf{q} \right) \\
\times &\mathscr{D}_0 \left(E - \frac{\mathbf{q}^2}{2M_\Xi}, \mathbf{q} \right) + \mathcal{C}_3^{(10)}(-y_0 y_1)\sqrt{\frac{3}{2}} M_n \\
\times &\int^{\Lambda_{\rm reg}} \frac{{\rm d}^3\mathbf{q}}{(2\pi)^3} t_B\left(\mathbf{q},\mathbf{k};E\right) \frac{g_3(\Lambda_{\rm reg})}{\Lambda_{\rm reg}^2} \\
\times &\mathscr{D}_0 \left(E - \frac{\mathbf{q}^2}{2M_\Xi}, \mathbf{q} \right),
\end{aligned} \tag{54}
$$

and

$$
\begin{aligned}
t_B\left(\mathbf{p},\mathbf{k};E\right) = (-y_0 y_1) \Bigg[&\mathcal{C}_2^{(10)} S_n \left(E - \frac{\mathbf{k}^2}{2M_n} - \frac{\mathbf{p}^2}{2M_\Xi}, \mathbf{p}+\mathbf{k} \right) \\
&- \mathcal{C}_3^{(10)} \sqrt{\frac{3}{2}} M_n \frac{g_3(\Lambda_{\rm reg})}{\Lambda_{\rm reg}^2} \Bigg] \\
- \mathcal{C}_2^{(10)}(-y_0 y_1) &\int^{\Lambda_{\rm reg}} \frac{{\rm d}^3\mathbf{q}}{(2\pi)^3} t_A\left(\mathbf{q},\mathbf{k};E\right) S_n \\
&\left(E - \frac{\mathbf{p}^2}{2M_\Xi} - \frac{\mathbf{q}^2}{2M_n}, \mathbf{p}+\mathbf{q} \right) \\
\times &\mathscr{D}_1 \left(E - \frac{\mathbf{q}^2}{2M_n}, \mathbf{q} \right) + \mathcal{C}_3^{(10)}(-y_0 y_1)\sqrt{\frac{3}{2}} M_n
\end{aligned}
$$

$$
\times \int^{\Lambda_{\rm reg}} \frac{{\rm d}^3\mathbf{q}}{(2\pi)^3} t_A\left(\mathbf{q},\mathbf{k};E\right) \frac{g_3(\Lambda_{\rm reg})}{\Lambda_{\rm reg}^2}
$$

$$
\times \mathscr{D}_1 \left(E - \frac{\mathbf{q}^2}{2M_n}, \mathbf{q} \right). \tag{55}
$$

Here, $\mathcal{C}_2^{(11)} = 1/2$, $\mathcal{C}_2^{(10)} = -\sqrt{3/2}$ are spin–isospin recoupling coefficients for diagrams with two-body interaction only, and $\mathcal{C}_3^{(11)} = \mathcal{C}_3^{(10)} = 1$ are those with the three-body contact interaction. Upon renormalization using the wavefunction renormalization constant $\mathcal{Z}_{\Xi n}$ (cf. Eq. (17)), and projecting on to the S-wave, the above amplitudes lead to Eqs. (13) and (14).

References

1. S. Petschauer et al., Front. Phys. **8**, 12 (2020)
2. H.W. Hammer, S. König, U. van Kolck, Rev. Mod. Phys. **92**, 025004 (2020)
3. E. Hiyama, K. Nakazawa, Ann. Rev. Nucl. Part. Sci. **68**, 131–159 (2018)
4. A. Gal, E.V. Hungerford, D.J. Millener, Rev. Mod. Phys. **88**, 035004 (2016)
5. A. Gal, AIP Conf. Proc. **2249**, 030001 (2020)
6. H. Garcilazo, A. Valcarce, J. Vijande, Int. J. Mod. Phys. E **29**, 1930009 (2020)
7. L. Tolos, L. Fabbietti, Prog. Part. Nucl. Phys. **112**, 103770 (2020)
8. A.L. Watts et al., Rev. Mod. Phys. **88**, 021001 (2016)
9. J. Schaffner-Bielich, A. Gal, Phys. Rev. C **62**, 034311 (2000)
10. P. Demorest et al., Nature **467**, 1081–1083 (2010)
11. J. Antoniadis et al., Science **340**, 6131 (2013)
12. R.L. Jaffe, Phys. Rev. Lett. **38**, 195 (1977)
13. M. Oka, K. Shimizu, K. Yazaki, Phys. Lett. B **130**, 365 (1983)
14. B. Silvestre-Brac, J. Carbonell, C. Gignoux, Phys. Rev. D **36**, 2083 (1987)
15. U. Straub et al., Phys. Lett. B **200**, 241 (1988)
16. C. Nakamoto, Y. Suzuki, Y. Fujiwara, Prog. Theor. Phys. **97**, 761 (1997)
17. S.R. Beane et al. [NPLQCD Collaboration], Phys. Rev. Lett. **106**, 162001 (2011)
18. T. Inoue et al. [HAL QCD], Phys. Rev. Lett. **106**, 162002 (2011)
19. S.R. Beane et al. [NPLQCD Collaboration], Phys. Rev. D **85**, 054511 (2012)
20. P.E. Shanahan, A.W. Thomas, R.D. Young, Phys. Rev. Lett. **107**, 092004 (2011)
21. J. Haidenbauer, U.-G. Meissner, Phys. Lett. B **706**, 100 (2011)
22. T. Inoue et al. [HAL QCD Collaboration], Nucl. Phys. A **881**, 28 (2012)
23. K. Sasaki et al. [HAL QCD Collaboration], EPJ Web Conf. **175**, 05010 (2018)
24. Y. Yamaguchi, T. Hyodo, Phys. Rev. C **94**, 065207 (2016)
25. A. Francis et al., Phys. Rev. D **99**, 074505 (2019)
26. H. Garcilazo, A. Valcarce, Chin. Phys. C **44**, 104104 (2020)
27. J.K. Ahn et al. [KEK-PS E224 Collaboration], Phys. Lett. B **444**, 267 (1998)

600

Eur. Phys. J. Spec. Top. (2021) 230:579–601

28. B.H. Kim et al., Phys. Rev. Lett. **110**, 222002 (2013)
29. J.M. Lattimer, New Astron. Rev. **54**, 101 (2010)
30. D. Lonardoni, F. Pederiva, S. Gandolfi, Phys. Rev. C **89**, 014314 (2014)
31. D. Lonardoni et al., Phys. Rev. Lett. **114**, 092301 (2015)
32. B.P. Abbott et al. [LIGO Scientific and Virgo Collaboration], Phys. Rev. Lett. **119**, 161101 (2017)
33. H. Takahashi et al., Phys. Rev. Lett. **87**, 212502 (2001)
34. P. Khaustov et al. [AGS E885], Phys. Rev. C **61**, 054603 (2000)
35. S. Aoki et al. [KEK E176 Collaboration], Nucl. Phys. A **828**, 191 (2009)
36. K. Nakazawa et al., PTEP **2015**, 033D02 (2015)
37. E. Hiyama et al., Phys. Rev. C **78**, 054316 (2008)
38. T.F. Carames, A. Valcarce, Phys. Rev. C **85**, 045202 (2012)
39. H. Garcilazo, A. Valcarce, Phys. Rev. C **92**, 014004 (2015)
40. T.T. Sun et al., Phys. Rev. C **94**, 064319 (2016)
41. H. Garcilazo, A. Valcarce, Phys. Rev. C **93**, 034001 (2016)
42. H. Garcilazo, A. Valcarce, J. Vijande, Phys. Rev. C **94**, 024002 (2016)
43. I. Filikhin, V.M. Suslov, B. Vlahovic, Math. Model. Geom. **5**, 1–11 (2017)
44. E. Hiyama et al., Phys. Rev. Lett. **124**, 092501 (2020)
45. Y. Jin et al., Eur. Phys. J. A **56**, 135 (2020)
46. D.H. Wilkinson et al., Phys. Rev. Lett. **3**, 397 (1959)
47. L. Fabbietti,Nagae2018, *The 13th International Conference on Hypernuclear and Strange Particle Physics, Portsmouth USA, June 2018* (2018). https://www.jlab.org/conferences/hyp2018/program.html
48. A. Sanchez Lorente [PANDA Collaboration], Hyperfine Interact. **229**, 45 (2014)
49. S. Aoki et al., Nucl. Phys. A **644**, 365 (1998)
50. T. Tamagawa et al., Nucl. Phys. A **691**, 234 (2001)
51. J.K. Ahn et al., Phys. Lett. B **633**, 214 (2006)
52. M. Yamaguchi et al., Prog. Theor. Phys. **105**, 627 (2001)
53. E. Friedman, A. Gal, Phys. Rept. **452**, 89 (2007)
54. E. Hiyama et al., Prog. Theor. Phys. Suppl. **185**, 152 (2010)
55. J. Haidenbauer, U.-G. Meißner, S. Petschauer, Nucl. Phys. A **954**, 273 (2016)
56. K.W. Li, T. Hyodo, L.S. Geng, Phys. Rev. C **98**, 065203 (2018)
57. J. Haidenbauer, U.-G. Meißner, Eur. Phys. J. A **55**, 23 (2019)
58. M. Kohno, S. Hashimoto, Prog. Theor. Phys. **123**, 157 (2010)
59. Krishichayan et al., Phys. Rev. C **81**, 014603 (2010)
60. M.M. Nagels, T.A. Rijken, Y. Yamamoto, (2015). arXiv:1504.02634 [nucl-th]
61. T.A. Rijken, H.J. Schulze, Eur. Phys. J. A **52**, 21 (2016)
62. K. Sasaki et al. [HAL QCD Collaboration], Nucl. Phys. A **998**, 121737 (2020)
63. H. Garcilazo, A. Valcarce, Phys. Rev. Lett. **110**, 012503 (2013)
64. H. Garcilazo, A. Valcarce, T.F. Carames, J. Phys. G **41**, 095103 (2014)
65. H. Garcilazo, A. Valcarce, T.F. Carames, J. Phys. G **42**, 025103 (2015)
66. T. Hyodo, T. Hatsuda, Y. Nishida, Phys. Rev. C **89**, 032201 (2014)
67. U. Raha, Y. Kamiya, S.I. Ando, T. Hyodo, Phys. Rev. C **98**, 034002 (2018)
68. E. Braaten, H.W. Hammer, Phys. Rept. **428**, 259 (2006)
69. G.V. Skornyakov, K.A. Ter-Martirosyan, Sov. Phys. JETP **4**, 648 (1957)
70. G.V. Skornyakov, K.A. Ter-Martirosyan, Zh. Eksp. Teor. Fiz. **31**, 775 (1956)
71. G.V. Skornyakov, K.A. Ter-Martirosyan, Sov. Phys. JETP **31**, 775 (1956)
72. P.F. Bedaque, H.W. Hammer, U. Van Kolck, Phys. Rev. Lett. **82**, 463 (1999)
73. P.F. Bedaque, H.W. Hammer, U. Van Kolck, Nucl. Phys. A **676**, 357 (2000)
74. P.F. Bedaque, H.W. Hammer, U. van Kolck, Nucl. Phys. A **646**, 444 (1999)
75. D.B. Kaplan, Nucl. Phys. B **494**, 471 (1997)
76. D.B. Kaplan, M.J. Savage, M.B. Wise, Nucl. Phys. B **478**, 629 (1996)
77. D.B. Kaplan, M.J. Savage, M.B. Wise, Phys. Lett. B **424**, 390 (1998)
78. D.B. Kaplan, M.J. Savage, M.B. Wise, Nucl. Phys. B **534**, 329 (1998)
79. D.B. Kaplan, M.J. Savage, M.B. Wise, Phys. Rev. C **59**, 617 (1999)
80. U. van Kolck, Nucl. Phys. A **645**, 273 (1999)
81. P.F. Bedaque, H.W. Hammer, U. van Kolck, Phys. Rev. C **58**, 641 (1998)
82. M.C. Birse, J.A. McGovern, K.G. Richardson, Phys. Lett. B **464**, 169 (1999)
83. S. Beane et al., *Part of At the frontier of particle physics. Handbook of QCD*, vol. 1–3(2001), p. 133
84. G.S. Danilov, Zh. Eksp. Teor. Fiz. **40**, 498 (1961)
85. G.S. Danilov, Sov. Phys. JETP **13**, 349 (1961)
86. V. Efimov, Phys. Lett. B **33**, 563 (1970)
87. V.N. Efimov, Yad. Fiz. **12**, 1080 (1970)
88. V.N. Efimov, Sov. J. Nucl. Phys. **12**, 589 (1971)
89. V. Efimov, Nucl. Phys. A **210**, 157 (1973)
90. P. Naidon, S. Endo, Rept. Prog. Phys. **80**, 056001 (2017)
91. C.A. Bertulani, H.W. Hammer, U. Van Kolck, Nucl. Phys. A **712**, 37 (2002)
92. P.F. Bedaque, H.W. Hammer, U. van Kolck, Phys. Lett. B **569**, 159 (2003)
93. H.W. Hammer, Nucl. Phys. A **705**, 173 (2002)
94. S.I. Ando, U. Raha, Y. Oh, Phys. Rev. C **92**, 024325 (2015)
95. F. Hildenbrand, H.W. Hammer, Phys. Rev. C **100**, 034002 (2019)
96. S.-I. Ando, G.-S. Yang, Y. Oh, Phys. Rev. C **89**, 014318 (2014)
97. S.I. Ando, Y. Oh, Phys. Rev. C **90**, 037301 (2014)
98. G. Meher, U. Raha, Phys. Rev. C **103**(1), 014001 (2021). arXiv:2002.06511 [nucl-th]
99. C. Rappold et al. [HypHI Collaboration], Phys. Rev. C **88**, 041001 (2013)
100. A. Gal, H. Garcilazo, Phys. Lett. B **736**, 93 (2014)
101. H. Garcilazo, A. Valcarce, Phys. Rev. C **89**, 057001 (2014)

102. E. Hiyama, S. Ohnishi, B.F. Gibson, T.A. Rijken, Phys. Rev. C **89**, 061302 (2014)
103. I.R. Afnan, B.F. Gibson, Phys. Rev. C **92**, 054608 (2015)
104. N. Barnea et al., Phys. Rev. Lett. **114**, 052501 (2015)
105. J. Kirscher et al., Phys. Rev. C **92**, 054002 (2015)
106. L. Contessi et al., Phys. Lett. B **772**, 839–848 (2017)
107. J. Kirscher, E. Pazy, J. Drachman, N. Barnea, Phys. Rev. C **96**, 024001 (2017)
108. L. Contessi, N. Barnea, A. Gal, Phys. Rev. Lett. **121**, 102502 (2018)
109. L. Contessi et al., Phys. Lett. B **797**, 134893 (2019)
110. Q. Chen et al., Phys. Rev. C **77**, 054002 (2008)
111. A.C. Phillips, Nucl. Phys. A **107**, 209 (1968)
112. P.A. Zyla et al. [Particle Data Group], PTEP **2020**(8), 083C01 (2020)
113. V. Bernard, N. Kaiser, U.-G. Meissner, Int. J. Mod. Phys. E **4**, 193 (1995)
114. H.W. Griesshammer, Nucl. Phys. A **744**, 192 (2004)
115. E. Wilbring, Ph.D Dissertation, Efimov Effect in Pionless Effective Field Theory and its Application to Hadronic Molecules, Univ. of Bonn (2016)
116. M.T. Yamashita, L. Tomio, T. Frederico, Nucl. Phys. A **735**, 40 (2004)
117. M. Hjorth-Jensen, M.P. Lombardo, U. van Kolck, An advanced course in computational nuclear physics. Lect. Notes Phys. **936** (2017)
118. D.V. Fedorov, A.S. Jensen, Phys. Rev. Lett. **71**, 4103 (1993)
119. R.A. Minlos, L.D. Faddeev, Dokl. Akad. Nauk SSSR **141**, 1335 (1961)
120. R.A. Minlos, L.D. Faddeev, Sov. Phys. Doklady **6**, 1072 (1962)
121. S.D. Glazek, K.G. Wilson, Phys. Rev. Lett. **89**, 230401 (2002) [**Erratum-ibid. 92, 139901 (2004)**]
122. S.D. Glazek, K.G. Wilson, Phys. Rev. B **69**, 094304 (2004)
123. A. LeClair, J.M. Roman, G. Sierra, Phys. Rev. B **69**, 020505 (2004)
124. A. LeClair, J.M. Roman, G. Sierra, Nucl. Phys. B **675**, 584 (2003)
125. A. LeClair, J.M. Roman, G. Sierra, Nucl. Phys. B **700**, 407 (2004)
126. D. Sornette, Phys. Rept. **297**, 239 (1998)